THESIS APPROVED BY

December 5. 2025

Date

Garrett A. Soukup, Ph.D., Major Advisor

Signed by:
Dr. David He
33E6CD9838D24C8...

David Z.Z. He, Ph.D., Committee Member

Signed by:
Dr. Litao Tao
514E72979FA84CF...

Litao Tao, Ph.D., Committee Member

Signed by:
Dr. Sade Kosoko-Lasaki
CADA1B5359E2414...

Sade Kosoko-Lasaki, M.D., Committee Member

A. Barron Breland, D.M.,
Dean, Graduate School

INVESTIGATION OF SENSORY CELL-SPECIFIC CHANGES IN GENE EXPRESSION IN MICRORNA-183 FAMILY KNOCKOUT MOUSE INNER EAR FROM BULK RNA SEQUENCING ANALYSIS.

By

Tobi Sara Atale

A MASTER'S THESIS

Submitted to the Faculty of the Graduate School of Creighton University in Partial Fulfillment of the Requirements for the Degree of Master of Science in the Department of Biomedical Sciences

Omaha, NE

August 25, 2025

ABSTRACT

Hearing loss impacts a significant portion of the human population. According to a 2018 report by the World Health Organization, about 466 million people worldwide, including 34 million children, experience disabling hearing loss. Recent advances in molecular biology have emphasized the pivotal role of microRNAs in regulating gene expression during the development and maintenance of the inner ear. These small non-coding RNAs influence key biological processes such as cell differentiation, apoptosis, and oxidative stress, which are essential for maintaining cochlear function and protecting auditory sensory cells. Changes in microRNA expression have been linked to different types of hearing loss, including age-related, noise-induced, and genetic or congenital. Our lab focuses on the miRNA-183 family, which includes three microRNAs: miR-183, miR-96, and miR-182. These microRNAs are expressed in sensory neurons and sensory epithelial hair cells. The miRNA-183 family has been linked to hereditary deafness in both humans and mice.

To investigate the potential roles of the miR-183 family in the inner ear, our research team conducted bulk RNA sequencing to compare newborn mouse inner ear tissues from wild-type versus miR-183 family knockout (KO) mice. Bulk RNA sequencing revealed numerous gene expression changes in the cochlear sensory epithelium and spiral ganglion due to miR-183 family loss-of-function. However, these changes in gene expression represent an average across the entire tissue and do not provide insight into cell-specific gene expression. To address this, I combined existing bulk RNA sequencing data with publicly available single-cell RNA sequencing data from the gene Expression Analysis Resource (gEAR) database to obtain cellular resolution. First, we compiled a list of differentially expressed predicted miRNA target genes,

either upregulated or downregulated, that changed in expression by at least 20% due to miR-183 family KO. From this list, we selected the top 25 highly expressed genes and the top 25 most changed genes, whether upregulated or downregulated. Subsequently, we generated heatmaps in gEAR to visualize and explore cell-specific gene expression patterns of these genes across different cochlear cell types and spiral ganglion neurons.

Results revealed 31 Genes of Interest (GOIs) based on hair cell specificity in the sensory epithelia at P1 and 37 GOIs based on developmental expression in the spiral ganglion from E14 to P1, representing a total of 60 individual genes. Concurrently, the human gene database GeneCards was used to gather information on the names, functions, and associated diseases, including hearing loss, of these 60 genes. Furthermore, DAVID (Database for Annotation, Visualization, and Integrated Discovery) was also utilized to perform Gene Ontology (GO) analysis, which enhanced the classification of these genes and helped identify patterns related to their potential functions in the mouse inner ear. After this thorough analysis, a total of 19 GOIs were identified: *Egr1, Nnat, Plod2, Rims3, Cntn1, Idh2, Cfl1, Anp32b, Palld, Hspa2, Kif5a, Map1b, Zbtb20, Plag1, Prkce, Amotl2, Slc44a2, Dcx, and Sncb.* These 19 genes stood out due to their expression patterns after KO, their cell-specific expression in single-cell analysis data, their potential involvement in hearing loss-related diseases, and their specific cellular processes (i.e., GO terms). Out of these 19 GOIs, four genes including *Egr1, Nnat, Plod2, and Rims3* were selected as easily validatable targets to investigate cell-specific changes in expression resulting from miR-183 family KO by immunostaining. Collectively, these findings could advance hearing research by illustrating the impact of miR-183 family KO on specific genes involved in the development and maintenance of the inner ear and their potential effects on hearing loss.

DEDICATION

I am pleased to dedicate this thesis to my husband for his steadfast support in helping me reach my goals. I also thank my mother, whose prayers and support have been invaluable, especially in caring for my girls while I focused on writing. Thank you.

ACKNOWLEDGEMENT

It's been quite a journey, and first and foremost, I would like to thank God Almighty, who has been my anchor throughout it all. I am deeply grateful to my mentor, Dr. Garrett Soukup, for his scientific expertise, unwavering support, guidance, and honest feedback, all of which have guided me along the way. His mentorship and immense patience have helped me grow into a better scientist and sharpen my critical thinking skills. I also sincerely appreciate the members of my advisory committee—Dr. Sade Kosoko-Lasaki, Dr. David He, and Dr. Litao Tao—for their expertise and constructive criticism, which have been vital to the success of this work. I would also like to acknowledge Dr. Jian Zuo, who first welcomed me as a master's student in his lab and paved the way for me to develop a deep appreciation for scientific research. Lastly, I am extremely grateful to all the faculty, staff, and students of the Biomedical Sciences Department at Creighton University. You are all incredible, and I am so happy to have met each of you.

TABLE OF CONTENTS

ABSTRACT i
DEDICATION iii
ACKNOWLEDGEMENT iv
TABLE OF CONTENTS v
LIST OF FIGURES vi
LIST OF TABLES vii
ABBREVIATIONS viii
Chapter 1: Introduction and Background 1
MicroRNA Biogenesis and Function 1
Biological Effects of miRNAs and Hearing Loss 3
MicroRNAs in Inner Ear Development and Function 3
Dicer KO Mouse Models 5
miR-183 family in Hair Cell and Spiral Ganglion Neuron Development 8
miR-96 and Hearing Loss in Humans 13
miR-183 Family KO Mouse Models 14
Results from Previous Bulk RNA Sequencing Analysis 15
Lack of Cellular Resolution in Bulk RNA Sequencing Data 17
Chapter 2: Research Methods 19
miR-183/96/182 KO Mouse Model 19
Bulk RNA Sequencing Analysis of KO vs WT Tissues 19
Generation of Gene Lists from Bulk RNA Sequencing Data 21
Gene Expression Analysis Using gEAR 21
Gene Function and Gene Ontological Analysis 22
Chapter 3: Results and Conclusions 24
Analysis of Sensory Epithelia Target Gene Expression 24
Analysis of Spiral Ganglion Target Gene Expression 34
Chapter 4: Discussion 70
Chapter 5: References 74

LIST OF FIGURES

Figure 1.1. Canonical pathway of miRNA biogenesis ---------- 2

Figure 1.2. Defects in inner ear morphogenesis and sensory epithelial development of Pax2-Cre Dicer KO mice. ---------- 7

Figure 1.3. Neurosensory miR-183 family. ---------- 10

Figure 1.4. Neurosensory miR-183 family expression ---------- 12

Figure 3.1. Upregulated and downregulated miR-183-targeted DEGs in SE ---------- 26

Figure 3.2. Heatmaps and Venn diagram of the top 25 upregulated miR-183-targeted DEGs in SE. ---------- 30

Figure 3.3 Heatmaps and Venn diagram of the top 25 downregulated miR-183-targeted DEGs in SE. ---------- 33

Figure 3.4 Upregulated and downregulated miR-183-targeted DEGs in SG ---------- 35

Figure 3.5 Heatmaps and Venn diagram of the top 25 upregulated miR-183-targeted DEGs in SG. ---------- 37

Figure 3.6 Heatmaps and Venn diagram of the top 25 downregulated miR-183-targeted DEGs in SG. ---------- 39

Figure 3.7: Venn diagrams of top 25 genes and GOIs in SE and SG ---------- 41

LIST OF TABLES

Table 1.1. Summary of expressed and differentially expressed genes in miR-183 family KO versus WT mouse inner ear tissues. -- 16

Table 3.1. Summary of gene expression observations from SE and SG analyses ------------------ 43

Table 3.2. Function of GOIs and associated hearing disorders in SE and SG --------------------- 46

Table 3.3. Gene ontology enrichment analysis of 37 genes in SE----------------------------------- 63

Table 3.4. Gene ontology enrichment analysis of 31 genes in SG----------------------------------- 65

Table 3.5. Selection of antibodies for Egr1, Nnat, Plod2, and Rims3 in the SE and SG ---------- 69

ABBREVIATIONS

Abbreviation	Definition
Bulk RNA-seq	Bulk RNA sequencing
C57BL/6	C57Black6
DAVID	Database for Annotation, Visualization, and Integrated Discovery
DEG	Differentially expressed gene
gEAR	gene Expression Analysis Resource
GO	Gene Ontology
GOI	Gene of Interest
HC	Hair cell
ICC	Immunocytochemistry
IHC	Inner hair cell
KO	Knockout
miR-183 family	microRNA 183 family
miR/miRNA	microRNA
Myo1c	Myosin-1c
Myo5b	Myosin-5b
nt	Nucleotide
OCTs	Other cell types
OHC	Outer hair cell
P0	Postnatal day 0
scRNA-seq	Single-cell RNA-sequencing

SE	Sensory epithelia
SG	Spiral ganglion
SGN	Spiral Ganglion Neuron
WHO	World Health Organization
WT	Wild-Type

Chapter 1: Introduction and Background

MicroRNA Biogenesis and Function

miRNAs are non-coding RNAs produced from primary transcripts through nuclear and cytoplasmic ribonuclease processing that play essential roles in regulating gene expression. Most miRNAs are transcribed from DNA sequences into primary miRNAs and then processed into precursor and mature forms (O'Brien, 2018). In the nucleus, pri-miRNA transcripts are synthesized by RNA Polymerase II (RNA Pol II) and subsequently processed into pre-miRNA by the microprocessor complex, which includes an RNA-binding protein called DiGeorge Syndrome Critical Region 8 (DGCR8) and the ribonuclease III enzyme DROSHA (O'Brien, 2018). DGCR8 recognizes an N6-methyladenylated GGAC and other motifs within the pri-miRNA, while DROSHA cleaves the pri-miRNA duplex at the base of its characteristic hairpin structure (O'Brien, 2018). After pre-miRNAs are generated, they are exported to the cytoplasm via an Exportin 5 (XPO5)/RAN-GTP complex and then processed by the RNase III endonuclease enzyme DICER. This processing removes the terminal loop, creating a mature miRNA duplex (O'Brien, 2018). Once loaded into Argonaute (AGO) proteins (AGO1-4 in mammals), one strand of the miRNA duplex is retained as the guide strand to form the RNA-induced silencing complex (RISC). In contrast, the other strand, known as the passenger strand, is expelled (Suzuki, 2023). Most studies have shown that miRNAs bind to a specific sequence in the 3′ Untranslated Region (UTR) of their target mRNAs to induce translational repression, as well as mRNA deadenylation and decapping (O'Brien, 2018). miRNAs guide the interaction of RISC with target mRNAs through "seed pairing" interactions involving nucleotides 2-8, known as the seed sequence. By inhibiting translation and/or accelerating mRNA degradation, miRNAs fine-tune gene expression. A single miRNA may repress hundreds of predicted target mRNAs **(Fig. 1.1).**

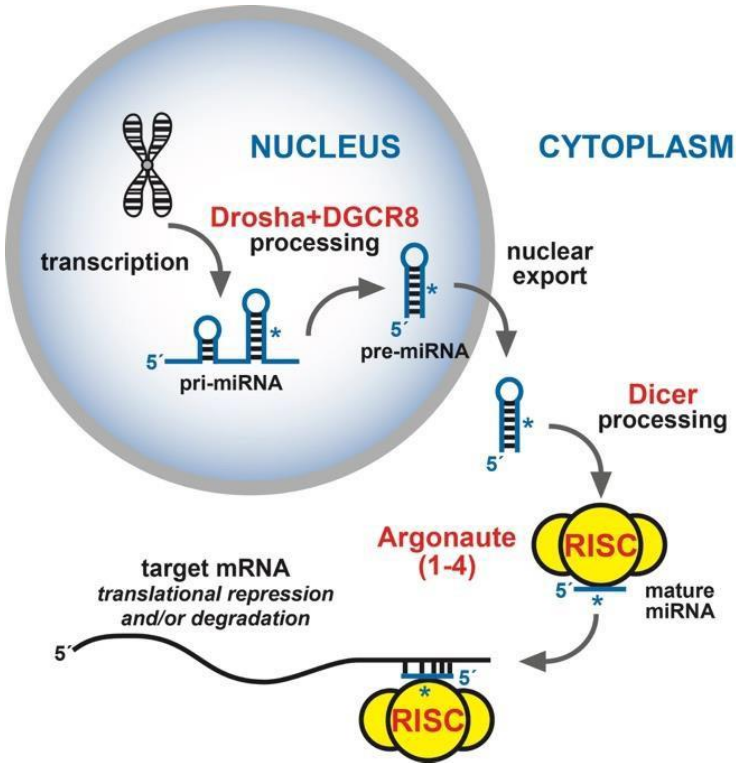

Figure 1.1. Canonical pathway of miRNA biogenesis.

In the nucleus, pre-miRNA transcripts are produced from pri-miRNA by DROSHA and DGRC8, then exported to the cytoplasm via Exportin 5. Once in the cytoplasm, DICER cleaves the stem-loop from the pre-miRNA, producing mature miRNA that associates with RISC. This miRNA guides RISC to bind to specific mRNAs through seed sequence pairing, leading to either inhibition of translation or degradation of mRNA.

Biological Effects of miRNAs and Hearing Loss

The ear is a complex structure consisting of the outer, middle, and inner ear. For the auditory system to function properly, the development of all these parts must be highly organized. Any disruptions in this process can lead to hearing loss or other impairments, such as dizziness, tinnitus, and loss of balance (Lavoro, 2022). Several external and internal factors—including noise exposure, ototoxic medications, aging, environmental influences, or genetics—have been associated with hearing loss (Lavoro, 2022). Despite these associations, there has been a recent surge in interest within the auditory community to understand the role of microRNAs (miRNAs) in inner ear development and hearing loss (Mittal, 2018). MicroRNAs are 21–24-nucleotide noncoding RNAs that function as post-transcriptional regulators of gene expression. Changes in the expression of microRNAs have been linked to various types of hearing loss, including age-related, noise-induced, and genetic or congenital. Previous research has shown that increased levels of miR-34a are found in the cochlea, auditory cortex, and plasma of C57BL/6 mice during aging, accompanied by elevated hearing thresholds and a greater hair cell loss (Pang, 2016). Similarly, studies have demonstrated that miR-153 levels significantly increase after noise exposure compared to controls, and inhibiting miR-153 effectively reduces outer hair cell (OHC) loss following noise exposure (Wang, Q., 2021). Overall, miRNAs have been shown to play a significant role in inner ear development and thus may play a role in the development or prevention of hearing loss (Mittal, 2018).

MicroRNAs in Inner Ear Development and Function

Gene regulation by miRNAs plays a crucial role in development, physiology, and disease (Suzuki, 2023). MicroRNAs account for 1-2% of all genes in worms, flies, and mammals, and since each miRNA is predicted to regulate hundreds of targets, most protein-coding genes are believed to be under their control. In reality, nearly every biological process is regulated by miRNAs (Vidigal, 2015). Studies in zebrafish and mice have shown the role of miRNAs in the development and function of the inner ear. Whole-mount in situ detection in zebrafish embryos revealed that some miRNAs are expressed in hair cells of sensory epithelia (Wienholds, 2005). Likewise, analysis of the mouse inner ear indicates that miRNA expression is widespread, with about one-third of known miRNAs detected in the inner ear (Weston, 2006). Furthermore, targeted deletion of the miR-183 family caused dysfunctions in multiple sensory epithelia, including the retina, organ of Corti, vestibular organs, and olfactory epithelium in mice (Fan, 2017). Additionally, several knockout studies suggest that many conserved miRNAs are dispensable for animal development or viability (Vidigal, 2015). miR-183 family KO mice show ciliogenesis disruption, implying that the formation of cilia, a critical step in the final differentiation of sensory receptor cells, is likely controlled by the miR-183 family of miRNAs. Defects in kinocilium extension were also observed in hair cells of the organ of Corti and vestibular organs (Fan, 2017). Moreover, it has been proposed that miRNAs could be used in the future for inner ear hair cell regeneration and therapeutic applications (Rudnicki, 2012). Additionally, previous studies in zebrafish demonstrated that the miR-183 family was upregulated during hair cell regeneration after ototoxic damage and that its inhibition decreased the regeneration process (Kim, 2018).

Dicer KO Mouse Models

Studies using conditional Dicer knockout mouse models demonstrate the crucial role of microRNAs in inner ear development. Dicer plays a pivotal role in miRNA biogenesis by cleaving pre-miRNA hairpins into mature, functional miRNAs that regulate gene expression. Deletion of Dicer in *Pax2-Cre* expressing mice caused developmental defects that possibly led to late embryonic death around E18.5 (Soukup, 2009). Comparing the normal inner ear **(Fig. 1.2A)** with the conditional Dicer knockout inner ear (CKO) **(Fig. 1.2B)** reveals a significant reduction in inner ear development in the KO (Soukup, 2009). In the vestibular and auditory organs, there are six sensory epithelia: the anterior, horizontal, and posterior cristae (AC, HC, and PC, respectively), utricular (U) and saccular (S) maculae, and the organ of Corti that runs along the cochlea (CO) (Fig. 1.2A). In **Fig. 1.2B**, the conditional Dicer KO mice show a notable truncation of most inner ear structures at E17.5. Although the KO inner ear has a well-developed posterior crista and canal, the horizontal crista and canal, as well as the anterior crista, are always absent **(Fig. 1.2B).** The anterior canal is either missing or greatly reduced, with a smaller utricle always present **(Figs. 1.2B and 1.2C).** A small saccule is sometimes visible, and the cochlea lacks coils **(Figs. 1.2B and 1.2D).** Overall, it has been shown that conditional Dicer KO in the developing mouse inner ear causes major morphogenic, histogenic, and innervation defects, including a lack of innervation in developing hair cells of the posterior crista and cochlea (Soukup, 2009). Similarly, *Atoh1-Cre* conditional *Dicer1* knockout (CKO) mice (*Atoh1-Cre;Dicer1*$^{flox/flox}$) were generated to investigate the function of miRNAs in hair cell development and maintenance. In situ hybridization (ISH) shows that miR-183 expression is largely depleted in *Dicer1* CKO inner ear hair cells by postnatal day 18 (P18) compared to control inner ear (Weston, 2011). Additional immunostaining of myosin VIIa and phalloidin staining of F-actin revealed a reduction in basal

OHCs and some apical OHCs in the *Dicer1* CKO at P28. These findings suggest that hair cell miRNA depletion leads to a gradual loss of OHCs from the base to the apex, indicating that miRNAs are essential for cochlear hair cell maintenance and survival (Weston, 2011).

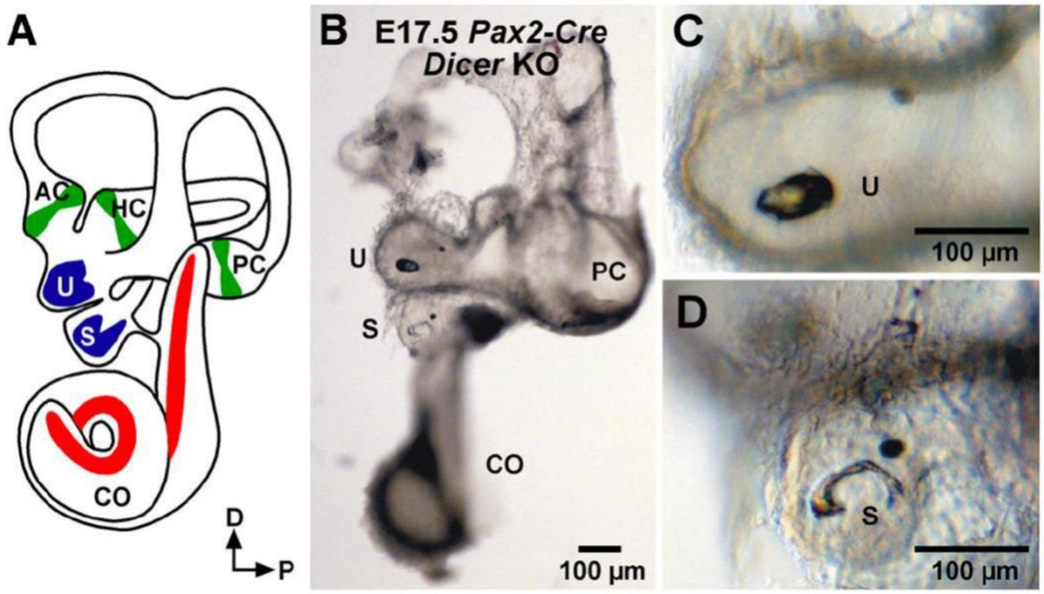

Figure 1.2. Defects in inner ear morphogenesis and sensory epithelial development of Pax2-Cre Dicer KO mice.

(A) Illustration of a typical inner ear showcasing the anterior, horizontal, and posterior cristae (AC, HC, and PC), along with the utricular (U) and saccular (S) maculae, and the organ of Corti in the cochlea (CO). Arrows indicate dorsal (D) and posterior (P) directions across all images. ***(B)*** Morphology of an E17.5 *Pax2-Cre Dicer* KO mouse inner ear. ***(C)*** Reduced utricle is visible in the Dicer KO. ***(D)*** Small saccule with a potentially misshapen otoconial mass.

miR-183 Family in Hair Cell and Spiral Ganglion Neuron Development

The miR-183 family plays a vital role in both sensory neurons and sensory epithelial hair cells and has been implicated in various diseases, including deafness, neurological disorders, autoimmune diseases, and cancer (Banks, 2020). miR-96 was the first human miRNA identified in this cluster, followed by miR-182 and miR-183 a year later (Mahmoodian-Sani, 2017). These three miRNAs are located next to each other, with approximately a 4 kb span between miR-96 and miR-182, and are transcribed as a long primary transcript (Mahmoodian-Sani, 2017). The vertebrate miR-183 family gene cluster is situated on a 1–4 kb DNA segment between the genes encoding Nuclear Respiratory Factor 1 (*Nrf1*) and Ubiquitin-conjugating Enzyme E2 H (*Ube2h*). The miRNAs are produced from a common untranslated primary transcript **(Fig. 1.3A)** (Pierce, 2008). The miR-183 family member sequence is highly conserved across vertebrate and invertebrate deuterostome species. This family may also include homologous miRNAs in protostome animals, which diverged from deuterostomes about 600 million years ago, such as miR-263a/b in *Drosophila* and miR-228 in *Caenorhabditis elegans* **(Fig. 1.3B)** (Pierce, 2008). Likewise, the miR-183 family members share a high degree of similarity within the seed sequence, which is responsible for recognizing target transcripts. Slight differences are seen in the second nucleotide of miR-183 and the eighth nucleotide of miR-182, highlighted in yellow **(Fig. 1.3B).** Studies suggest that mutations in miR-96 can cause both loss-of-function (LOF) and gain-of-function (GOF) effects. A mutation in pre-miR-96 in humans has been linked to progressive hereditary deafness (Mahmoodian-Sani, 2017) **(Fig. 1.3C).** Overall, the critical role of the miR-183 family in sensory cell development, maintenance, and function is well established. However, understanding the precise mechanisms involved remains difficult due to the many genes and pathways miRNAs potentially regulate, as well as the various levels of expression and regulation of miR-183 family members and their targets across different cell types. Computational predictions suggest that miRNAs regulate over one-third of human gene transcripts (Jin 2009). Bioinformatic analysis using TargetScanMouse 6.2 estimated there are 1,616 unique and shared predicted target genes of the miR-183 family in the mouse genome, representing about 6.6% of the 24,396 mouse genes **(Fig. 1.3D).**

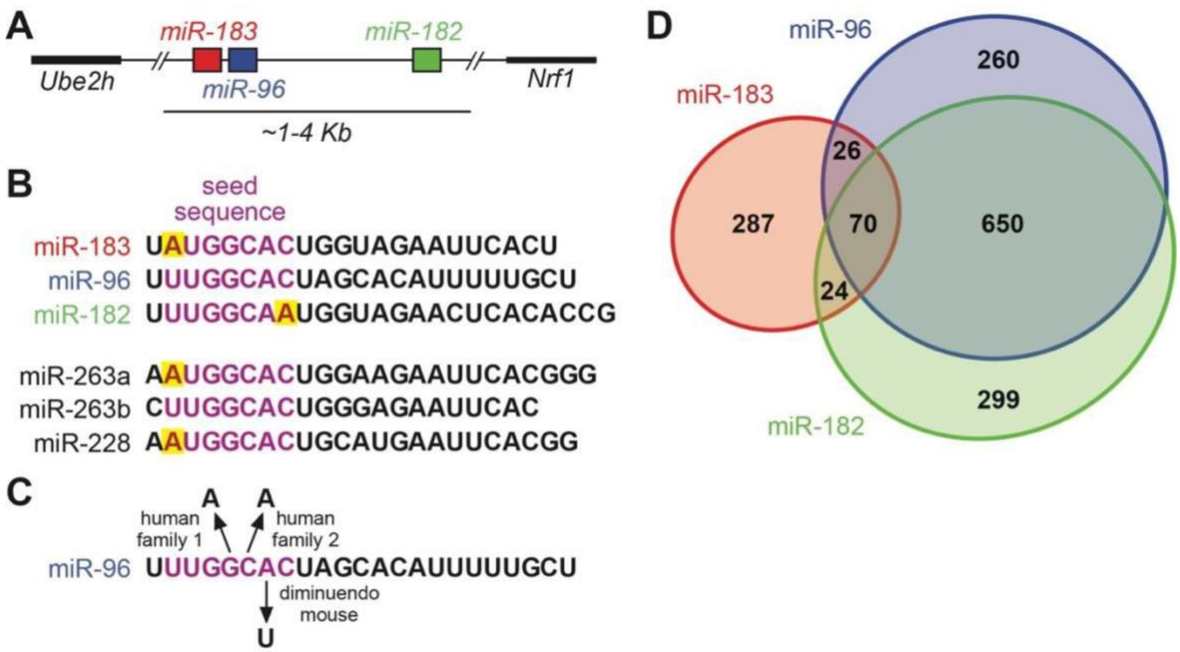

Figure 1.3. Neurosensory miR-183 family.

(A) miR-183, miR-96, and miR-182 are generally situated within a ~1–4 Kb segment of a large intergenic region between Ube2h and Nrf1 genes. (***B)*** miR-183 family sequences show a high degree of similarity, especially within the seed sequences (nucleotides 2–8; magenta); yellow highlighting indicates differences in seed sequences; miR-183 family homologs include fruit fly miR-263a/b and nematode worm miR-228. ***(C)*** Mutations in miR-96 sequences are observed in human families (G or C substituted with A) and mice (A substituted with C). ***(D)*** The area-proportional Venn diagram illustrates the number of 1616 collective transcripts predicted to be targeted by one or more of the three miRNAs using TargetScanMouse 7.2

To further investigate the role of the miR-183 family, *Li et al.* performed functional studies in zebrafish (2010). They injected fertilized zebrafish eggs with synthesized miR-96 and miR-182. Immunostaining for hair cells demonstrated that many embryos injected with either miR-182 or miR-96 developed an increased number of hair cells compared to controls. Conversely, knockdown of members of the miR-183 family consistently resulted in fewer hair cells (Li, 2010). Similarly, a mouse mutant induced by ENU (N-ethyl-N-nitrosourea), called diminuendo, which has a single base change in the seed region of miR-96, caused heterozygous mice to show progressive hearing loss and hair cell defects. Meanwhile, homozygous mice showed no cochlear responses (Lewis, 2009). A more recent study using two mouse lines with the same seed region miR-96 mutations found in humans revealed that these mutations cause profound deafness in homozygous mice; the effects in heterozygotes varied, highlighting the role of gain-of-function in novel target regulation for microRNA mutant phenotypes (Lewis, 2024). Additionally, the miR-183 family is highly expressed in specific sensory cell types in the eye, nose, and inner ear (Li, 2010). Whole-mount ISH with locked nucleic acid (LNA) performed across hair cell development from embryonic day E12.5 to E16.5 revealed miR-183 family expression in all sensory ganglia and inner ear epithelia at E16.5 (Weston, 2011). Correspondingly, ISH shows the expression of the miR-183 family in the embryonic mouse nervous system and sensory organs (**Fig. 1.4A)** (Banks, 2020). Furthermore, ISH detected miR-96 expression in sensory epithelia and sensory neurons of the postnatal day 0 (P0) wild-type FVB mouse inner ear **(Fig. 1.4B)** (Banks, 2020). miR-96 is found in hair cells (HCs) and spiral ganglion (SG) neurons of the organ of Corti (OC) within the cochlea, as well as in HCs of vestibular sensory epithelia, including posterior, anterior, and horizontal cristae (PC, AC, HC), and the utricular (U) and saccular (S) maculae **(Fig. 1.4B).**

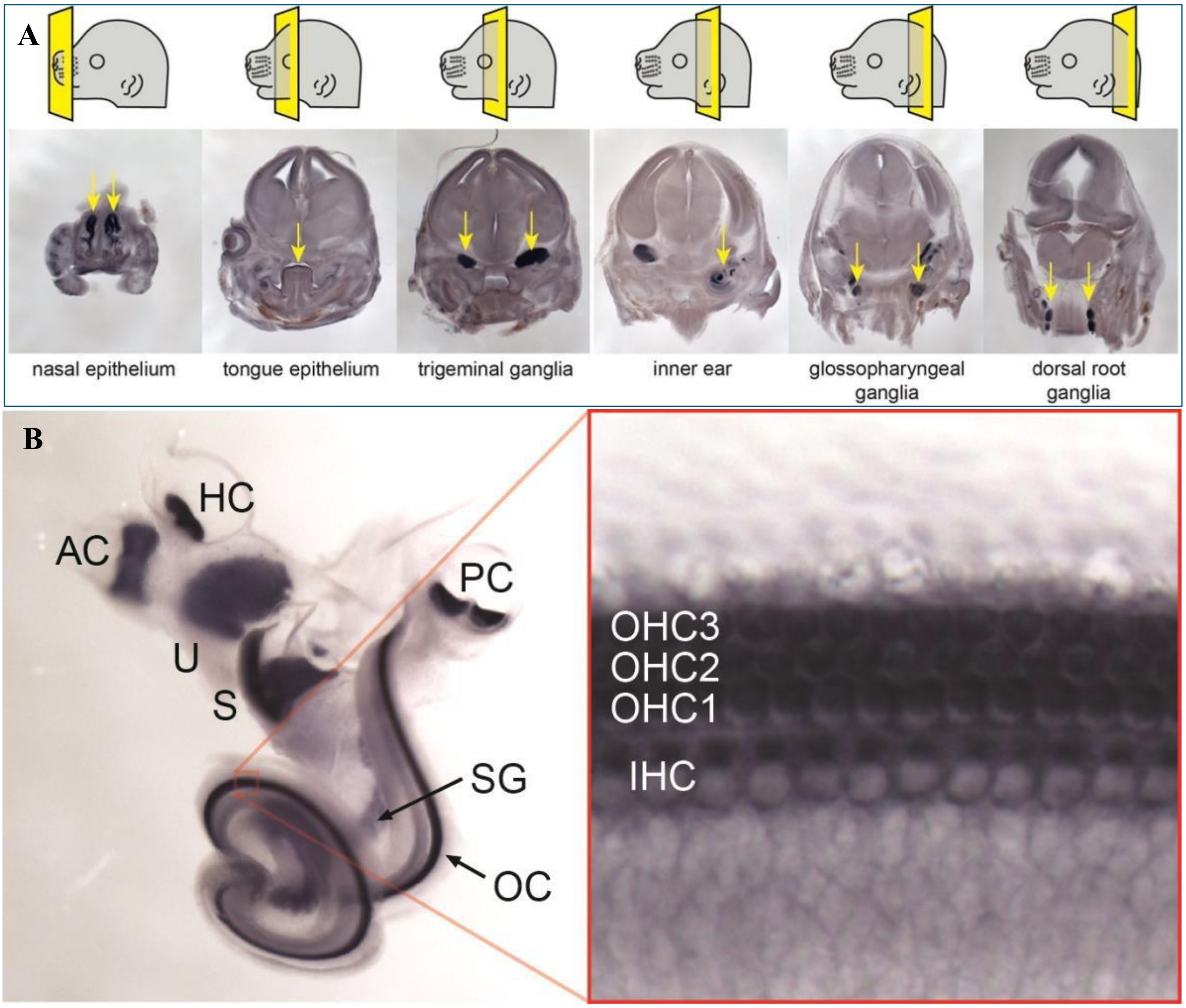

Figure 1.4. Neurosensory miR-183 family expression.

(A) Cross-sectional analysis of wild-type FVB mouse head indicates the approximate locations of miR-183 expression in the nasal and tongue epithelia, trigeminal ganglia, inner ear sensory epithelia and ganglia, glossopharyngeal ganglia, and dorsal root ganglia***, (B)*** miR-96 expression in the sensory epithelia (SE) and spiral ganglion (SG) of the inner ear in postnatal day 0 (P0) wild-type FVB mice; PC (posterior cristae) AC (anterior cristae), HC (horizontal cristae), OC (organ of Corti), U (utricle), S (saccule), OHC1, 2, 3 (three rows of outer hair cells), IHC (one row of inner hair cells) *miR-96 and Hearing Loss in Humans*

miR-96, part of the miR-183 microRNA family, plays a vital role in regulating gene expression in hair cells, which are essential for normal hearing (Mencía, 2009). Mencía et al have shown that point mutations in the seed region of miR-96, expressed in inner ear hair cells, cause autosomal dominant, progressive hearing loss. They identified an autosomal dominant deafness locus (*DFNA50*) on 7q32 in a Spanish family with postlingual, progressive, nonsyndromic all-frequency hearing loss (Mencía, 2009). They discovered a G-to-A transition at position 13 in one allele of miR-96, miR-96(+13 G>A), which replaced the fourth nucleotide within the conserved 7-nucleotide seed region of the mature sequence (Mencía, 2009). This mutation was not found in normal-hearing Spanish controls, leading to the conclusion that miR-96 mutations caused the *DFNA50* hearing loss in this family (Mencía, 2009). Another study found that point mutations within miR-96 lead to non-syndromic inherited hearing loss in an Italian family by disrupting pre-miRNA processing (Soldà, 2011). They showed that altered pre-miRNA secondary structure impaired mature miR-96 production, indirectly affecting the regulation of its targets and suggesting that even a quantitative shift in miR-96 levels can cause deafness (Soldà, 2011). These findings highlight the importance of miR-96 and the miR-183 family altogether in human hearing loss.

miR-183 Family KO Mouse Models

Given the importance of miR-183 family expression in inner ear development and function, multiple knockout (KO) models have been studied. These KO studies have shed light on the vital roles of these miRNAs. Mice lacking individual or all members of the miR-183 family exhibit severe hearing loss, hair cell abnormalities, and synaptic defects. Three different KO mouse models have been studied: miR-182 KO, miR-183/96 KO, and miR-183/96/182 KO. Prior research shows miR-182 is highly expressed in the mammalian retina, suggesting important roles in retinal development and function (Jin, 2009). Consequently, miR-182 deficient mice were created to study miR-182 expression in both embryonic and postnatal eyes (Jin, 2009). ISH with LNA-modified probes revealed strong miR-182 expression in embryonic and P3 inner retinas, notably in the ganglion cell layer (Jin, 2009). Additionally, Xiang et al. (2017) generated miR-183/96 KO mice, demonstrating that the absence of both miR-183 and miR-96 leads to defective cone nuclear polarization and progressive retinal degeneration, reaffirming the role of the miR-183 family in sensory neurons. Lastly, knocking out the entire miR-183/96/182 gene cluster in mice via homologous recombination resulted in mice with impairments across multiple sensory systems—vision, hearing, balance, and smell—mainly due to severe defects in sensory receptor terminal differentiation (Fan 2017). Additionally, a Gene-Trap (GT) designed to inactivate the 183/96/182 cluster gene caused homozygous mutant mice to exhibit severe congenital hearing loss and cochlear hair cell defects in maturation, alignment, and bundle formation, suggesting that the microRNA-183/96/182 cluster is essential for stereociliary bundle formation and cochlear sensory hair cell function (Geng, 2018).

Results from Previous Bulk RNA Sequencing Analysis

To explore the role of the miR-183 family in the cochlear sensory epithelium (SE) and spiral ganglion (SG), our team conducted high-throughput bulk RNA sequencing (bulk RNA-seq) to examine changes in gene expression between knockout (KO) and wild-type (WT) tissues (Soukup lab, unpublished). Computational analysis revealed that the mouse genome has approximately 24,396 genes, with about 1,616 being miRNA target genes, representing roughly 6.6% **(Table 1.1).** In the SE, 8,617 differentially expressed genes (DEGs) with an FPKM (Fragments per Kilobase per Million Mapped reads) greater than 10 were identified, including both targeted and non-targeted genes. In the SG, 7,971 DEGs met this criterion. Of these, 969 target genes were found in the SE (11.2%), and 1,022 in the SG (12.8%) **(Table 1.1)**, both exceeding the predicted 6.6%. The analysis further identified genes with at least 20% expression change, either up or down. In the SE, 127 target genes were identified among 1,025 downregulated genes (about 12.4%), while in the SG, 45 target genes were identified among 402 downregulated genes (around 11.2%) **(Table 1.1)**, both above the expected 6.6%. For upregulated genes, 110 target genes were identified among 1,018 upregulated genes in the SE (10.8%), and 193 target genes were identified among 771 upregulated genes in the SG (25.0%) **(Table 1.1).** These data show higher-than-expected enrichment based on the 6.6% target prediction, with the SG showing notably greater enrichment than the SE (25% vs 10.8% vs 6.6%). Although **Table 1.1** lists both non-target and target genes identified via bulk RNA-seq, the upregulated target genes are particularly noteworthy because miRNAs usually suppress gene expression; thus, their targets are more likely to be upregulated following KO.

Table 1.1. Summary of expressed and differentially expressed genes in miR-183 family KO versus WT mouse inner ear tissues.

	Genes[1]	Non-Target Genes[2]	Target Genes[2]	Target Gene Representation[3]
Mouse Genome	24396	22780	1616	6.6%
Sensory Epithelium	8617	7648	969	11.2%
Upregulated[4]	1018	908	110	10.8%
Downregulated[4]	1025	898	127	12.4%
Spiral Ganglion	7971	6949	1022	12.8%
Upregulated[4]	771	578	193	25.0%
Downregulated[4]	402	357	45	11.2%

[1]Total genes in the mouse genome versus those expressed at >10 FPKM.

[2]Genes predicted to not be/be miR-183/96/182 target genes.

[3]Percentage of predicted target genes among total genes.

[4]Genes upregulated or downregulated by 20% in miR-183 family KO compared to wild-type.

Lack of Cellular Resolution in Bulk RNA Sequencing Data

While the bulk RNA-seq dataset has helped identify differentially expressed miR-183-KO targeted genes in the SE and SG, it is limited in capturing differences between individual cells within the population, making cellular resolution difficult. Bulk-RNA sequencing measures average gene expression across thousands or millions of cells but loses information about cell-to-cell variability. However, scRNA-seq captures gene expression at the single-cell level, even though each cell receives fewer reads. Besides, bulk RNA-seq is relatively low-cost and technically less challenging to perform than scRNA-seq. Because scRNA-seq provides a more comprehensive understanding of cellular diversity, it enables the extraction of cellular resolution from previous bulk RNA-seq data. However, performing scRNA-seq is technically challenging, as the miR-183-KO mutation causes neonatal lethality in C57BL/6 mice, requiring cell genotyping before sequencing. This conflicts with the timeline of sample preparation and data analysis, as scRNA-seq requires live cells. This limitation has prompted the exploration of publicly available single-cell RNA sequencing (scRNA-seq) data in gEAR to add cellular resolution to bulk RNA-seq data, since microRNA loss can cause substantial changes in gene expression. To address this, publicly available scRNA-seq data from wild-type (WT) P1 mice were searched in gEAR to serve as a template for deriving cellular-resolution (i.e., cell-specific gene expression) from bulk RNA-seq data. The process involved selecting the top 25 highly expressed genes and the top 25 most changed genes (upregulated or downregulated) for miR-183 family targets in the SE and SG. Heatmaps generated in gEAR enabled analysis of cell-specific patterns across cochlear cell types and spiral ganglion neurons. From this, 31 and 37 genes were identified in the SE and SG, respectively, for a total of 60 genes of interest (GOIs). These genes were then examined in the human gene database, GeneCards, to obtain information on their names, functions, and associations with hearing loss-related diseases. To further refine these genes, gene ontology (GO) analysis from DAVID (Database for Annotation, Visualization, and Integrated Discovery) confirmed their cellular components, molecular functions, and biological processes. Ultimately, four GOIs—Egr1, Nnat, Plod2, and Rims3—were selected based on their expression patterns after KO, cell-specific expression in scRNA-seq data, potential involvement in hearing-related diseases, and associated cellular processes (i.e., GO terms). These genes are promising candidates for studying cell-specific expression changes in miR-183 family KO, supported by literature data on their immunostaining potential. The following sections will describe the methods, present the results, and discuss potential implications for hearing research.

Chapter 2: Research Methods

miR-183/96/182 KO Mouse Model

Animal care and handling in this study complied with protocols approved by the Institutional Animal Care and Use Committee of Creighton University. The miR-183/96/182 knockout mouse line was generated by the Sanger Institute (Prosser et al. 2012) and maintained in a C57Bl/6N genetic background by line breeding mice that are heterozygous for the knockout allele. Animals were genotyped by PCR analysis of tail DNA using a common forward primer (5'-TTGGCAGGAAGGTGGCTTGT) combined with a KO-specific reverse primer (5'-GAACAGCCCTCAGGGGTTGA) or WT-specific reverse primer (5'-AAGGTGCTCGCGGATCTGTC), which each produce a KO-specific 695 bp product or WT-specific 384 bp product. Newborn animals were anesthetized by inhalation of 20% Isoflurane diluted in propylene glycol and prepared for dissection of inner ear tissues by thoracotomy and transcardiac perfusion with phosphate-buffered saline (PBS; 10 mM Na_2HPO_4, 1.7 mM KH_2PO_4, 137 mM NaCl, 2.7 mM KCl, pH7.4).

Bulk RNA Sequencing Analysis of KO vs WT Tissues

Cochleae from newborn mice were rapidly dissected in cold PBS to isolate spiral ganglion or sensory epithelial tissue from each ear. Tissue from the left and right ears were combined for each biological sample and stored in RNAlater stabilization reagent (ThermoFisher Scientific) until corresponding tail biopsies were genotyped. Spiral ganglion tissue from three biological samples for each genotype (WT, heterozygous, and KO) were selected for individual RNA isolation and sequencing (i.e. Nine individual samples, three for each genotype). Sensory epithelial tissues from three biological samples for each genotype were pooled for RNA isolation and sequencing (i.e. three pooled samples, one for each genotype). Following mechanical tissue homogenization, total RNA was purified from individual or pooled samples using a *mir*Vana miRNA Isolation Kit (ThermoFisher Scientific). Total RNA was dissolved in 50 μL of RNase-free water. The quantity and quality of each total RNA sample was determined using a Nanodrop ND-1000 UV spectrophotometer (ThermoFisher Scientific) and an Agilent 2100 Bioanalyzer.

Total extracted RNA from individual or pooled samples for each genotype were submitted for sequencing and analysis by the Genomics Core Facility at the University of Nebraska Medical Center. Each sample was converted to a cDNA library using a Nextera Library Preparation Kit (Illumina) according to the manufacturer's protocol. The composition and concentration of cDNA libraries were assessed using an Agilent 2100 Bioanalyzer and a Qubit fluorometer (ThermoFisher Scientific) to ensure that fragments were within an appropriate size range for sequencing. Sequencing was performed using an Illumina HiSeq2500 Sequence Analyzer to acquire 50-bp paired-end reads. Each sample yielded >50 million total reads. RNAseq datasets were analyzed using Tuxedo Software (Oracle) on an x86_64-redhat-linux-gnu (64-bit) system. Paired-end reads were mapped to the mouse genome (mm10) using TopHat 2, and resulting alignment data were analyzed with Cufflinks (v 2.0.2) to assemble aligned RNAseq reads into transcripts. Transcript abundance is reflected as fragments per kilobase per million mapped reads (FPKM). To determine differential gene expression between genotypes for each sample, the mapped reads generated by HTSeq were analyzed by DESeq with a false discovery rate of 5%. RNA FPKM values for KO samples were compared to those for WT controls. Differentially expressed genes were also compared to the predicted target genes of the miR-183/96/182 family (TargetScanMouse 7.2).

Generation of Gene Lists from Bulk RNA Sequencing Data

RNA bulk-seq data were analyzed to identify target genes of the P0 miR-183 family KO that are upregulated and downregulated, with an FPKM value exceeding 10 (FPKM >10) in both the SE and SG of KO compared to WT. This gene list was further refined by choosing differentially expressed genes (DEGs) that showed at least a 20% change in expression (≥20%). Finally, the top 25 highly expressed genes and the top 25 most changed genes in expression were selected from either the P0 miR-183 KO upregulated or downregulated groups.

Gene Expression Analysis Using gEAR

The PubMed electronic database was used to search for primary literature containing scRNA-seq data of the purified C57BL/6 population of SG neurons and SE hair cells between E18.5 and near P0-P4. Fifteen relevant articles were identified. Data were extracted from two primary research articles with available scRNA-seq datasets in gEAR. The first, "Characterization of the development of the mouse cochlear epithelium at the single-cell level" (Kolla & Kelley *et al*., 2020), was chosen as the primary dataset for analyzing cellular resolution in the SE from bulk RNA-seq because the researchers performed scRNA-seq on mouse sensory epithelia at P1—close to P0—and characterized transcriptional profiles for specific HC or SC subpopulations. This helped identify specific genes highly expressed in the sensory epithelia, facilitating comparison with existing bulk RNA-seq data of P0 miR183-KO targeted genes. The second article, "Specification of neuronal subtypes in the spiral ganglion begins prior to birth in the mouse" (Sanders and Kelley, 2022), served as the primary dataset for analyzing cellular resolution in the SG from bulk RNA-seq because it profiled SGNs during prenatal development from E14 to P1 using scRNA-seq. Its results suggest that transcriptionally controlled events during prenatal development are responsible for the initial formation of all four adult SGN subtypes, offering insight into gene expression changes following miR-183 family KO, as early development is key for SGN maturation.

Using gEAR, multiple gene lists were generated using the “Create new gene list” function by pasting genes from the RNA bulk sequencing dataset in Step 1. In Step 2, the “Multi Gene Displays” tool was used to select a publicly available dataset of interest. Step 3 involved selecting the “plot type” and “analysis type”. In Step 4, the gene list created earlier in Step 1 was selected, and in Step 5, the plotting options were adjusted to produce various heatmaps.

Gene Function and Gene Ontological Analysis

The Human Gene Database, GeneCards, was used to manually search for each gene of interest (GOI) by entering its symbol in the search bar to retrieve information on its name, function, and associated diseases, including hearing disorders. After obtaining results, additional website features were used for further exploration. Furthermore, these GOIs were examined through searches on “Google Scholar” and “PubMed” to find relevant literature on their roles in inner ear development or hearing loss-related diseases.

Using DAVID, the gene list for the 31 GOIs in the sensory epithelia was entered into the "Enter gene list" field in Step 1. In Step 2, a drop-down menu appeared to select the identifier, and “Official_gene_symbol” was chosen, followed by selecting the species “Mus musculus.” In Step 3, the “Gene List” option was selected as the list type, and the list was submitted for analysis in Step 4. The "Annotation summary results” were generated, with a primary focus on Gene Ontology analysis. The “functional annotation chart” for each process—specifically “GOTERM_CellularComponent_Direct,” “GOTERM_BiologicalProcess_Direct,” and

“GOTERM_MolecularFunction_Direct”—was downloaded and saved as an Excel file for future analysis, which was later organized into a table. The same steps were repeated for the 37 GOIs in the spiral ganglion.

Chapter 3: Results and Conclusions

Analysis of Sensory Epithelia Target Gene Expression

The list of predicted miR-183 family target genes that changed expression by at least 20% (≥ 20%) in the SE included 110 upregulated and 127 downregulated differentially expressed genes (DEGs). These genes were input into gEAR to cross-reference with the publicly available scRNA-seq analysis dataset "P1, mouse, scRNA seq, cochlear epithelium" (Kolla & Kelley *et al.*, 2020). This dataset was selected because the research group performed scRNA-seq on the sensory epithelia of P1 mice to characterize transcriptional profiles of unique HC or SC subpopulations, allowing the comparison with existing bulk RNA-seq data of P0 miR183-KO targeted genes. Using the dataset in gEAR, a heatmap was generated to show raw expression values of the 110 upregulated genes **(Fig. 3.1A)**. Similarly, a heatmap was created to display raw expression values of the 127 downregulated genes **(Fig. 3.1C).** Many genes showed low expression (i.e. blue in color). To enhance visualization of genes that are changed in expression from one cell type to another, expression values were normalized to the mean expression value of all genes in each dataset to generate alternative heat maps **(Fig. 3.1B and D).** Still, many genes do not exhibit substantial changes in expression among different cell types. Therefore, both gene lists were further refined to include only the top 25 highly expressed genes (i.e., target genes with the highest expression levels) and the top 25 differentially expressed genes (i.e., target genes with the most change in expression) between KO and WT for either upregulated or downregulated genes.

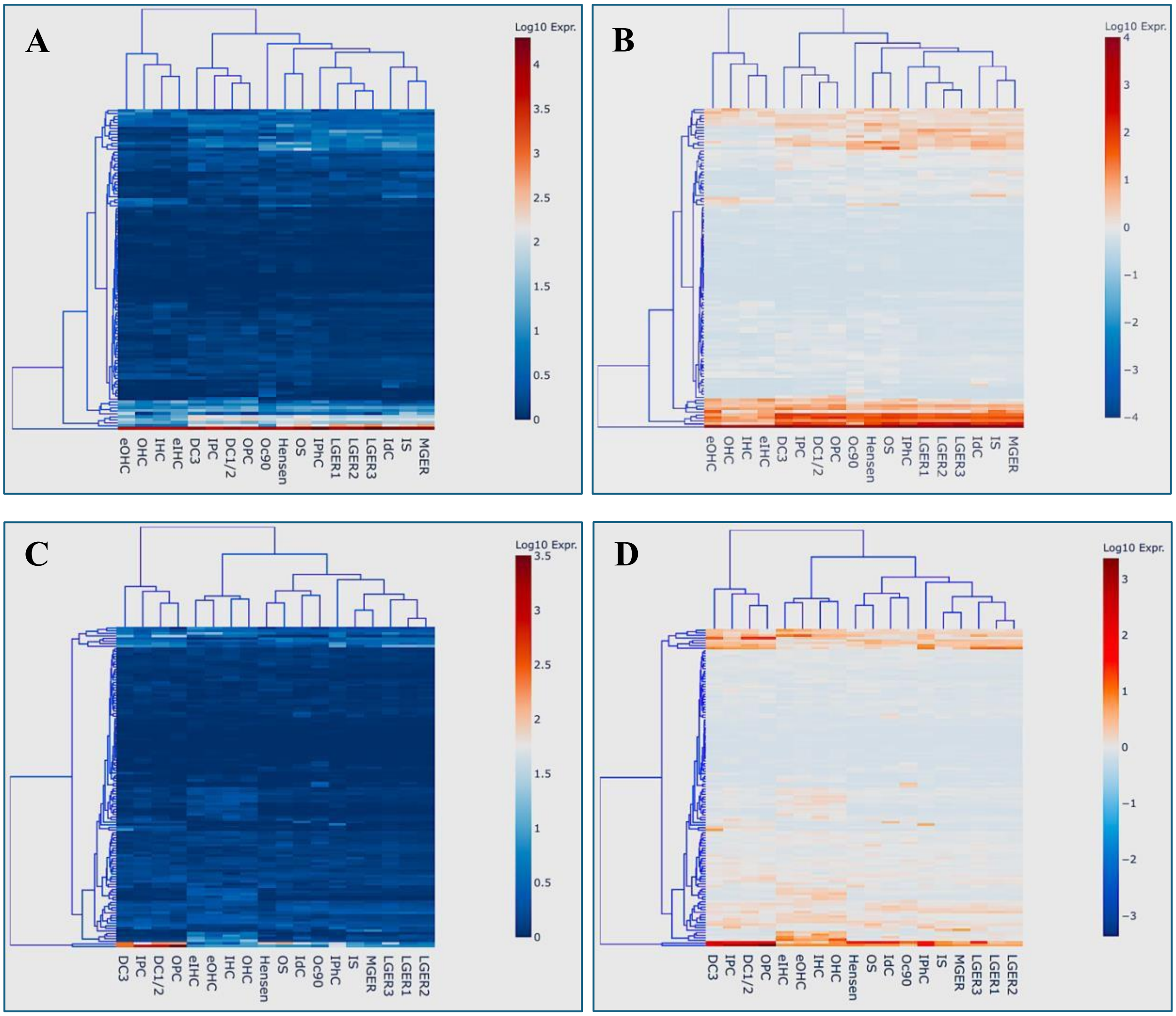
A
Log10 Expr.
eOHC OHC IHC eIHC DC3 IPC DC1/2 OPC Oc90 Hensen OS IPhC LGER1 LGER2 LGER3 IdC IS MGER
B
Log10 Expr.
eOHC OHC IHC eIHC DC3 IPC DC1/2 OPC Oc90 Hensen OS IPhC LGER1 LGER2 LGER3 IdC IS MGER
C
Log10 Expr.
DC3 IPC DC1/2 OPC eIHC eOHC IHC OHC Hensen OS IdC Oc90 IPhC IS MGER LGER3 LGER1 LGER2
D
Log10 Expr.
DC3 IPC DC1/2 OPC eIHC eOHC IHC OHC Hensen OS IdC Oc90 IPhC IS MGER LGER3 LGER1 LGER2

Figure 3.1. Upregulated and downregulated miR-183-targeted DEGs in SE.

Each heatmap shows expression values (log_{10}-transformed) for different genes (y-axis) in different cell types (x-axis) with hierarchical clustering by both expression value and cell type. ***(A)*** Raw expression values for 110 upregulated genes. ***(B)*** Mean normalized expression values centered around zero for 110 upregulated genes. ***(C)*** Raw expression values for 127 downregulated genes. ***(D)*** Mean normalized expression values centered around zero for 127 downregulated genes. Cell types include developing supporting cells (*DC1/2*: Dieter Cells from rows 1 and 2; *DC3*: Dieter Cells from row 3; *Hensen*: Hensen Cells; *IPC*: Inner Pillar Cells; *IPhC*: Inner Phalangeal Cells; *IS*: Inner Sulcus Cells; *IdC*: Interdental Cells; *OPC*: Outer Pillar Cells; *OS*: Outer Sulcus Cells; *Oc90*: Cells expressing Oc90); developing greater epithelial ridge cells (*LGER1*, *LGER2*, *LGER3*: Lateral Greater Epithelial Ridge Cells, groups 1, 2, and 3 respectively; *MGER*: Medial Greater Epithelial Ridge Cells); and developing sensory cells (*IHC*: Inner Hair Cells; *OHC*: Outer Hair Cells; *eIHC*: less mature developing inner hair cells; *eOHC*: less mature developing outer hair cells).

The heatmap in **Fig. 3.2A** illustrates the top 25 highly expressed genes among the 110 upregulated genes in the SE. Many genes show distinct expression patterns across different cell types. The primary focus was on the expression patterns of developing sensory cells (IHCs, OHCs, eIHCs, eOHCs) compared to developing greater epithelial ridge cells and supporting cells referred to as other cell types (OCTs). Therefore, cell specificity – namely genes with apparent lower or higher expression in HCs than OCTs within the dataset— was a key criterion for selecting genes of interest (GOIs). GOIs were also selected based on their apparent HC specificity in WT mice relative to their levels after miR-183 family KO, specifically whether expression increased or decreased after KO. The goal was to identify gene expression changes, especially for genes with lower expression in HCs in WT that increased after KO, reflecting the expected effects of miR-183 family KO in the inner ear. GOIs were grouped into three categories: (1) genes with lower expression in HCs than OCTs in WT, (2) genes with higher expression in HCs than OCTs in WT, and (3) genes with higher expression across all cell types. From **Fig. 3.2A**, five genes fell into category 1: *Zfp36l1, Idh2, Sdc2, and Pkp4* (IHC-specific) and *Nnat* (OHC-specific). Category 2 included *Dap*, while category 3 was comprised of *H3f3b, Cfl1, Paip2*, and *Anp32b* totaling 10 GOIs. Similarly, **Fig. 3.2B** depicts the top 25 most changed genes among the 110 upregulated genes in the SE. Focusing on HC specificity and expression levels before and after miR-183 family KO, five genes were identified in category 1: *Plod2, Idh2, Bace2, Nnat*, and *Egr1*; one gene in category 2: *Palld*; and one gene in category 3: *Hspa2* totaling seven GOIs. Notably, two genes (*Nnat and Idh2)* are listed among both the highly expressed and most changed GOIs and are therefore excluded from the total count, resulting in a total of five GOIs. Overall, between both analyses, 15 GOIs were identified. To better visualize the top 25 upregulated genes in the SE, a Venn diagram was created showing 22 unique genes among the top 25 highly expressed and top 25 most changed genes, with three overlapping genes (*Idh2, Plod2, Nnat*) **(Fig. 3.2C).**

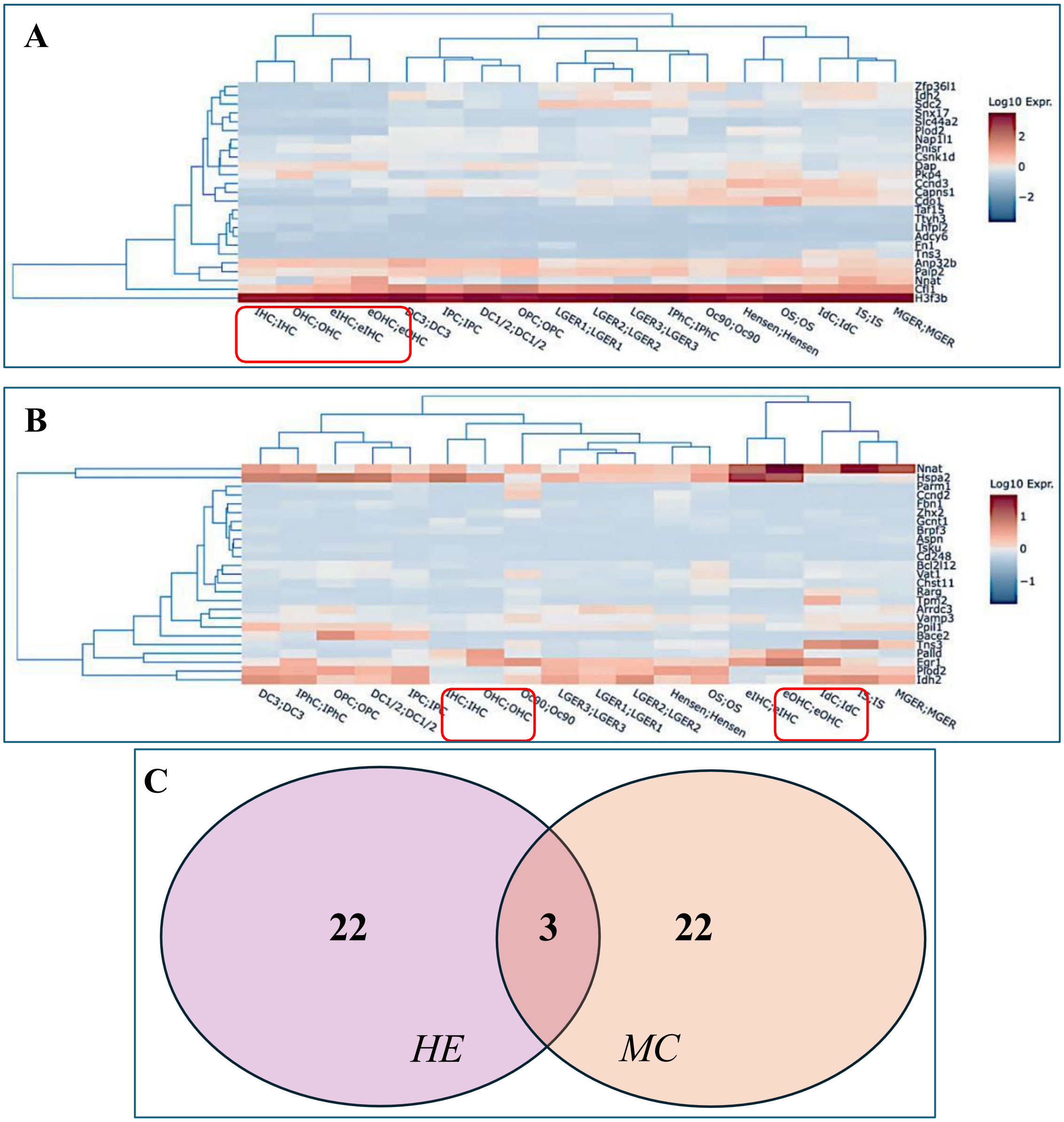
A
Zfp36l1
Idh2
Sdc2
Snx17
Slc44a2
Plod2
Nap1l1
Pnisr
Csnk1d
Dap
Pkp4
Ccnd3
Capns1
Cdo1
Taf15
Ttyh3
Lhfpl2
Adcy6
Fn1
Tns3
Anp32b
Palp2
Nnat
Cfl1
H3f3b
Log10 Expr.
2
0
−2
IHC;IHC
OHC;OHC
eIHC;eIHC
eOHC;eOHC
DC3;DC3
IPC;IPC
DC1/2;DC1/2
OPC;OPC
LGER1;LGER1
LGER2;LGER2
LGER3;LGER3
IPhC;IPhC
Oc90;Oc90
Hensen;Hensen
OS;OS
IdC;IdC
IS;IS
MGER;MGER
B
Nnat
Hspa2
Parm1
Ccnd2
Fbn1
Zhx2
Gcnt1
Brpf3
Aspn
Tsku
Cd248
Bcl2l12
Vat1
Chst11
Rarg
Tpm2
Arrdc3
Vamp3
Ppil1
Bace2
Tns3
Palld
Egr1
Plod2
Idh2
Log10 Expr.
1
0
−1
DC3;DC3
IPhC;IPhC
OPC;OPC
DC1/2;DC1/2
IPC;IPC
IHC;IHC
OHC;OHC
Oc90;Oc90
LGER3;LGER3
LGER1;LGER1
LGER2;LGER2
Hensen;Hensen
OS;OS
eIHC;eIHC
eOHC;eOHC
IdC;IdC
IS;IS
MGER;MGER
C
22
3
22
HE
MC

Figure 3.2. Heatmaps and Venn diagram of the top 25 upregulated miR-183-targeted DEGs in SE.

Each heatmap shows $\log_{10}$-transformed mean normalized expression values centered around zero for different genes (y-axis) in different cell types (x-axis) with hierarchical clustering by both expression value and cell type. ***(A)*** Top 25 highly expressed (HE) genes. ***(B)*** Top 25 most changed (MC) genes. Cell types are as listed in the legend to Fig. 3.1, with OHC, IHC, eOHC (immature OHC), and eIHC (immature IHC) indicated within red boxes. ***(C)*** Venn diagram showing unique and common genes among the top 25 HE and top 25 MC genes.

A similar analysis was performed for the 127 downregulated genes in the SE. **Figs. 3.3A and 3.3B** display heatmaps of the top 25 highly expressed genes and the top 25 most changed genes, respectively. Notably, the heatmap in **Fig. 3.3B** shows only 24 genes because one gene, *Srct1*, in the bulk RNA-seq dataset was absent from the single-cell RNA-seq dataset. As previously discussed, apparent HC specificity and HC expression levels in WT vs miR-183 family KO mice were used to analyze **Fig. 3.3A**. Four genes were identified as GOIs in category 1 (expression lower in HCs than in OCTs): *Trim2, Tsc22d3, Mbnl2, Rabgap1l*; six genes in category 2 (expression higher in HCs than in OCTs): *Myo5b, Prepl, Gramd1b, Rims3, Kif5a, Rnf157*; and two genes in category 3 (higher expression across all cell types): *Map1b* and *Mapk8ip1*, totaling 12 genes among the top 25 highly expressed. Similarly, **Fig. 3.3B** analysis revealed two GOIs in category 1: *Tsc22d3* and *Cntn1*; six in category 2: *Rims3, Kif5a, Rnf157, Amph, Cep85l, Ctnna2* (IHC-specific); and one in category 3: *Map1b*, totaling nine genes among the top 25 most changed. Five genes (*Rims3, Kif5a, Rnf157, Tsc22d3, Map1b*) appear in both lists of highly expressed genes and most changed genes. Therefore, there were a total of 16 GOIs among downregulated genes. Additionally, to better visualize the top 25 downregulated genes in the SE, a Venn diagram was created showing 17 unique genes among the top 25 highly expressed and most changed genes, along with eight overlapping genes (*Dcx, Kif5a, Map1b, Rims3, Rnf157, Rsp6ka3, Tle4, Tsc22d3*) **(Fig. 3.3C).**

Altogether, this investigation identified 31 GOIs in the SE that warrant further investigation for their potential direct or indirect roles in HC development or maintenance as miR-183 target genes.

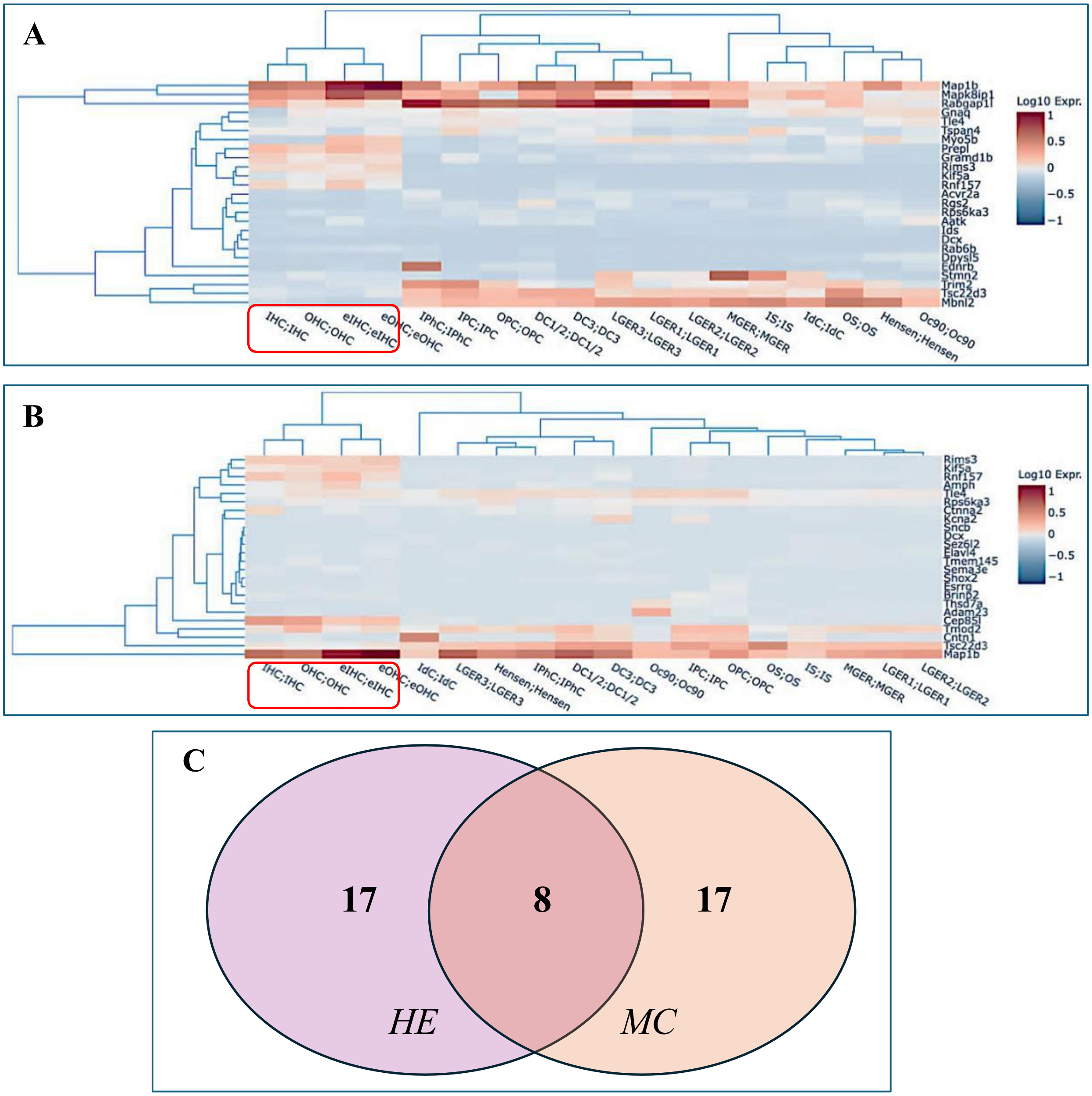
A
Map1b
Mapk8ip1
Rabgap1l
Gnaq
Tle4
Tspan4
Myo5b
Prepl
Gramd1b
Rims3
Kif5a
Rnf157
Acvr2a
Rgs2
Rps6ka3
Aatk
Ids
Dcx
Rab6b
Dpysl5
Ednrb
Stmn2
Trim2
Tsc22d3
Mbnl2
Log10 Expr.
1
0.5
0
−0.5
−1
IHC;IHC
OHC;OHC
eIHC;eIHC
eOHC;eOHC
IPhC;IPhC
IPC;IPC
OPC;OPC
DC1/2;DC1/2
DC3;DC3
LGER3;LGER3
LGER1;LGER1
LGER2;LGER2
MGER;MGER
IS;IS
IdC;IdC
OS;OS
Hensen;Hensen
Oc90;Oc90
B
Rims3
Kif5a
Rnf157
Amph
Tle4
Rps6ka3
Ctnna2
Kcna2
Sncb
Dcx
Sez6l2
Elavl4
Tmem145
Sema3e
Shox2
Esrrg
Brinp2
Thsd7a
Adam23
Cep85l
Tmod2
Cntn1
Tsc22d3
Map1b
Log10 Expr.
1
0.5
0
−0.5
−1
IHC;IHC
OHC;OHC
eIHC;eIHC
eOHC;eOHC
IdC;IdC
LGER3;LGER3
Hensen;Hensen
IPhC;IPhC
DC1/2;DC1/2
DC3;DC3
Oc90;Oc90
IPC;IPC
OPC;OPC
OS;OS
IS;IS
MGER;MGER
LGER1;LGER1
LGER2;LGER2
C
17
8
17
HE
MC

Figure 3.3 Heatmaps and Venn diagram of the top 25 downregulated miR-183-targeted DEGs in SE.

Each heatmap shows $\log_{10}$-transformed mean-normalized expression values centered around zero for different genes (y-axis) in different cell types (x-axis) with hierarchical clustering by both expression value and cell type. ***(A)*** Top 25 highly expressed (HE) genes. ***(B)*** Top 25 most changed (MC) genes. Cell types are as listed in the legend to Fig. 3.1, with OHC, IHC, eOHC (immature OHC), and eIHC (immature IHC) indicated within red boxes. ***(C)*** Venn diagram showing unique and common genes among the top 25 HE and top 25 MC genes.

Analysis of Spiral Ganglion Target Gene Expression

An analysis similar to that performed for the SE was also performed to analyze changes in gene expression observed in bulk RNA-seq analysis of spiral ganglion (SG) from miR-183 family KO mice compared to WT mice. The list of predicted miR-183 family target genes that changed in expression by at least 20% (≥20%) in the SG included 193 upregulated and 45 downregulated differentially expressed genes (DEGs) **(Table 1.1).** These genes were also input into gEAR to cross-reference with the publicly available scRNA-seq analysis dataset "Specification of neuronal subtypes in the spiral ganglion begins prior to birth in the mouse" (Sanders and Kelley, 2022). This dataset was chosen because the research group used scRNA-seq to profile SGN maturation across prenatal development between E14 and P1. Using this dataset, heatmaps illustrating the expression of the 193 upregulated genes **(Fig. 3.4A)** and 45 downregulated genes **(Fig. 3.4B)** were produced. Overall, many genes do not show distinct expression patterns among different cell types or developmental timepoints. Therefore, the two lists of genes were further refined to include only the top 25 highly expressed genes (i.e., target genes with the highest expression levels) and the top 25 most changed genes (i.e., target genes with the greatest change in expression level).

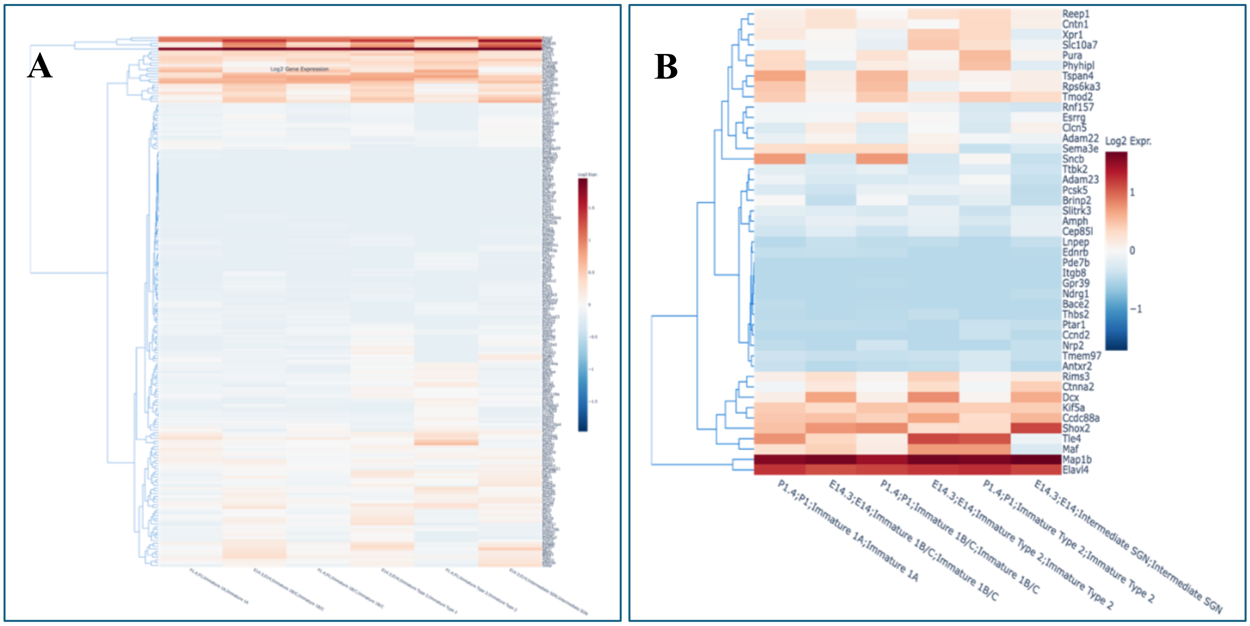

Figure 3.4 Upregulated and downregulated miR-183-targeted DEGs in SG.

Each heatmap shows $\log_2$-transformed mean normalized expression values centered around zero for different genes (y-axis) in different cell types (x-axis) with hierarchical clustering by expression value. ***(A)*** 193 upregulated genes. ***(B)*** 45 downregulated genes. SGN subtypes include Intermediate SGN, Immature Type 1A, 1B, 1C, and Type 2 neurons from embryonic mice at day 14 (E14; E14.3) and postnatal day 1 (P1; P1.4).

Fig. 3.5A and **Fig. 3.5B** display heatmaps of the top 25 highly expressed genes and the 25 most changed genes among the 193 upregulated genes in the SG, respectively. Unlike in the SE, where heatmaps were analyzed based on apparent HC specificity and expression levels in WT vs miR-183 family KO mice, the SG heatmaps were evaluated based on changes in gene expression from E14 to P1 (developmental age). GOIs were grouped into two categories: (1) genes decreasing in expression from E14 to P1 in the same cell subtype; and (2) genes increasing in expression from E14 to P1 in the same cell subtype. From **Fig. 3.5A**, six GOIs were identified in category 1: *Btg1, Nnat, Plod2, Ttyh3, Slc44a2,* and *Ccnd3*, and six GOIs in category (2): *Rcn2, Tmbim6, Pkp4, Pdia4, Pik3r1,* and *Paip2*, totaling 12 GOIs. Similarly, the analysis of **Fig. 3.5B** revealed ten genes in category (1): *Zbtb20, Nnat, Amotl2, Egr1, Chd2, Plod2, Crebrf, Kdm6a, Plag1*, and *Frmd6*, and four in category (2): *Rnf208, Prkce, Sh3bp4, and Amotl2*, totaling 14 GOIs. Notably, *Nnat*, *Plod2*, and *Amotl2* appear twice, leading to 23 total GOIs in this analysis of upregulated genes. Additionally, a Venn diagram **(Fig. 3.5C**) illustrates 23 unique genes in the top 25 highly expressed genes and the top 25 most changed genes, with two overlapping genes, *Nnat and Plod2.* Interestingly, *Nnat, Plod2, Pkp4*, *Paip2*, and *Erg1* are also GOIs that were identified in in the analysis of SE.

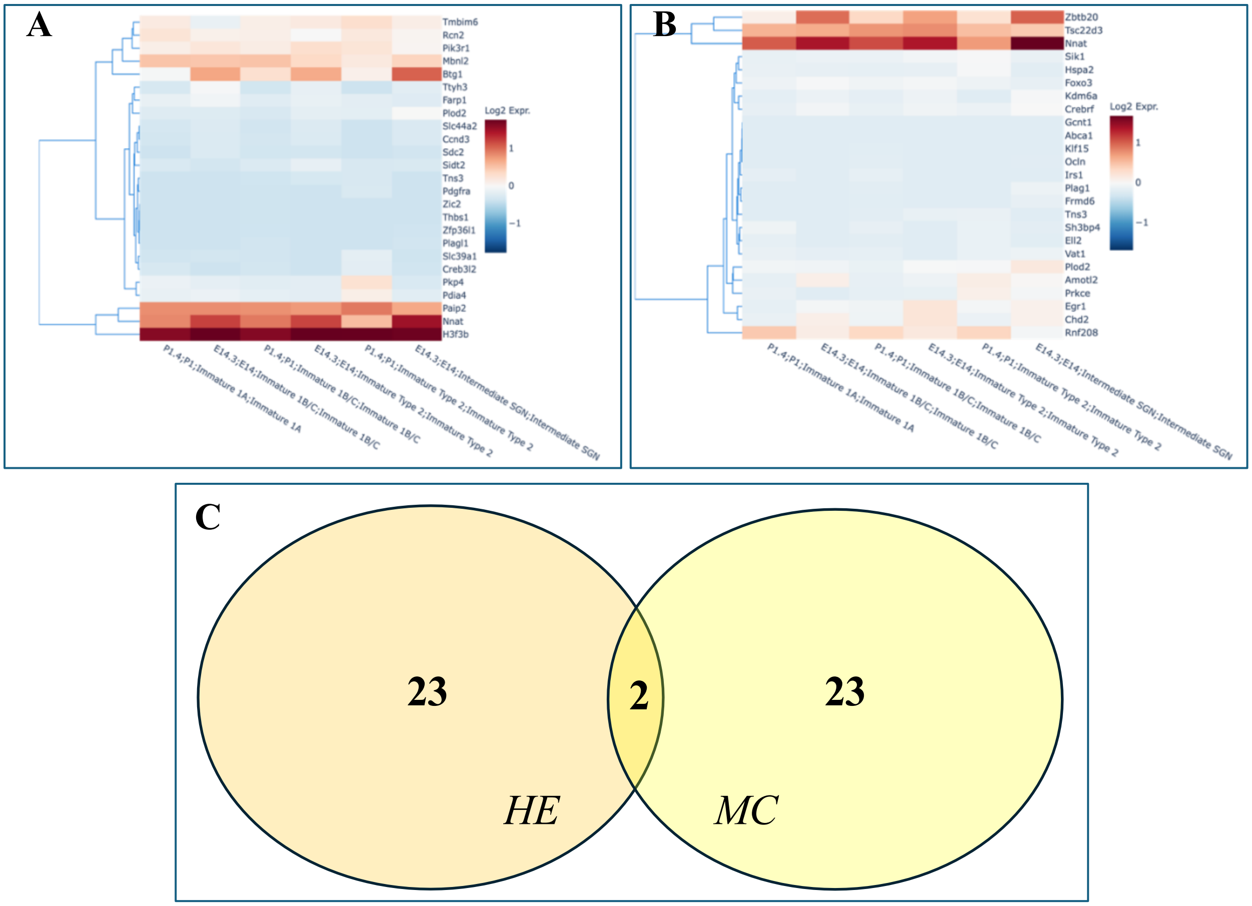

Figure 3.5 Heatmaps and Venn diagram of the top 25 upregulated miR-183-targeted DEGs in SG.

Each heatmap shows $\log_2$-transformed mean normalized expression values centered around zero for different genes (y-axis) in different cell types (x-axis) with hierarchical clustering by expression value. ***(A)*** Top 25 highly expressed (HE) genes. ***(B)*** Top 25 most changed (MC) genes. SGN subtypes are as indicated in the legend to **Fig. 3.4**. ***(C)*** Venn diagram illustrating unique and common genes among the top 25 HE and top 25 MC genes.

Focusing on the 45 downregulated genes in the SG, a heatmap was generated displaying the top 25 highly expressed genes **(Fig. 3.6A)** and the top 25 most changed genes **(Fig. 3.6B).** As before, the selection of each GOI was grouped into two categories. In **Fig. 3.6A**, three genes were identified in category 1: *Dcx, Ccdc88a,* and *Rims3*, while six were in category 2: *Sncb, Tmod2, Tle4, Maf, Tspan4,* and *Rps6ka3*, totaling 9 GOIs. The analysis in **Fig. 3.6B** resulted in three genes in category 1: *Dcx, Rims3,* and *Ctnna2*, and seven in category 2: *Pura, Cntn1, Brinp2, Adam23, Tle4, Tspan4*, and *Rps6ka3*, totaling 10 GOIs. Notably, *Dcx*, *Rims3*, *Tle4*, *Tspan4*, *and Rps6ka3* appear twice, leading to 14 total GOIs from this analysis of downregulated genes. To visualize the top 25 downregulated genes, a Venn diagram was created showing 11 unique genes in each list, with 14 overlapping genes (*Amph, Ccnd2, Cntn1, Dcx, Ednrb, Elavl4, Esrrg, Kif5a, Rims3, Rnf157, Rps6ka3, Sema3e, Tle4,* and *Tspan4)* **(Fig. 3.6C).** Interestingly, *Rims3*, *Ctnna2* and *Cntn1* are also GOIs that were identified in the analysis of SE.

Altogether, this investigation found a total of 37 GOIs in SG that warrant further investigation for their potential direct or indirect roles in neuronal cell development or maintenance as miR-183 target genes.

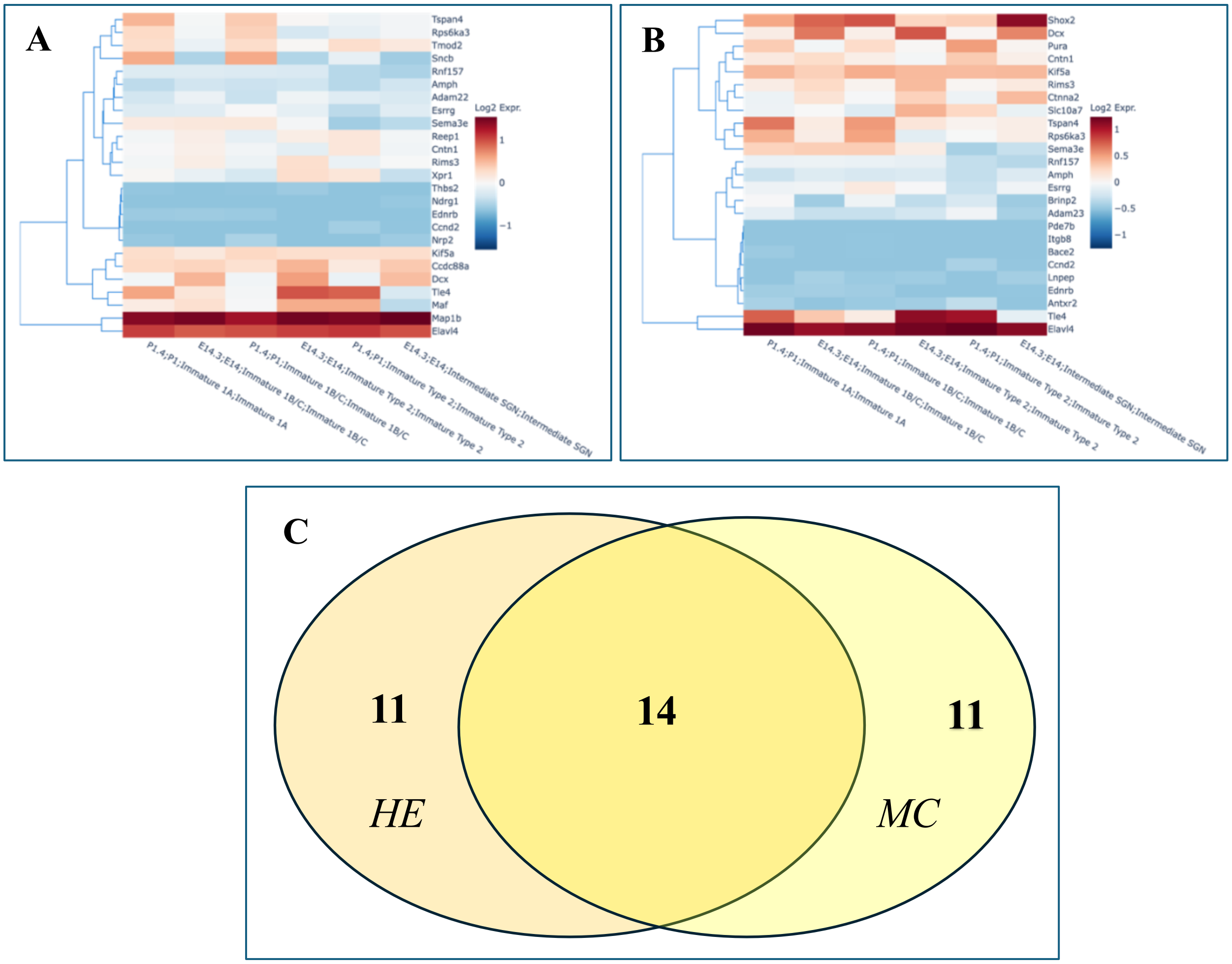

Figure 3.6 Heatmaps and Venn diagram of the top 25 downregulated miR-183-targeted DEGs in SG.

Each heatmap shows $\log_2$-transformed mean normalized expression values centered around zero for different genes (y-axis) in different cell types (x-axis) with hierarchical clustering by expression value. ***(A)*** Top 25 highly expressed (HE) genes. ***(B)*** Top 25 most changed (MC) genes. SGN subtypes are as indicated in the legend to **Fig. 3.4**. ***(C)*** Venn diagram illustrating unique and common genes among the top 25 HE and top 25 MC genes.

For a more comprehensive view of all top 25 genes and GOIs, a Venn diagram was created to display the total unique and common genes among top 25 genes for SE and SG, regardless of whether the genes were upregulated or downregulated, or highly expressed and/or most changed as predicted miR-183 target genes **(Fig. 3.7A).** In total, 53 and 49 genes were identified as unique to the SE and SG, respectively, while 35 genes were common to both tissue types including *Adam23, Amph, Bace2, Brinp2, Ccnd2, Ccnd3, Cntn1, Ctnna2, Dcx, Ednrb, Egr1, Elavl4, Esrrg, H3f3b, Kif5a, Map1b, Mbnl2, Nnat, Paip2, Pkp4, Plod2, Rims3, Rnf157, Rps6ka3, Sdc2, Sema3e, Sncb, Tle4, Tmod2, Tns3, Tsc22d3, Tspan4, Ttyh3, Vat1, Zfp36l1*. An additional Venn diagram for GOIs identified from analysis of SE or SG illustrates that the 31 GOIs in SE and 37 GOIs in SG include eight genes in common, *Cntn1, Ctnna2, Egr1, Paip2, Plod2, Pkp4, Nnat, and Rims3* **(Fig. 3.7B).** Therefore, a total of 60 individual GOIs were identified, the dysregulation of which may affect HC or SGN development and maintenance in miR-183 family knockout mouse inner ear.

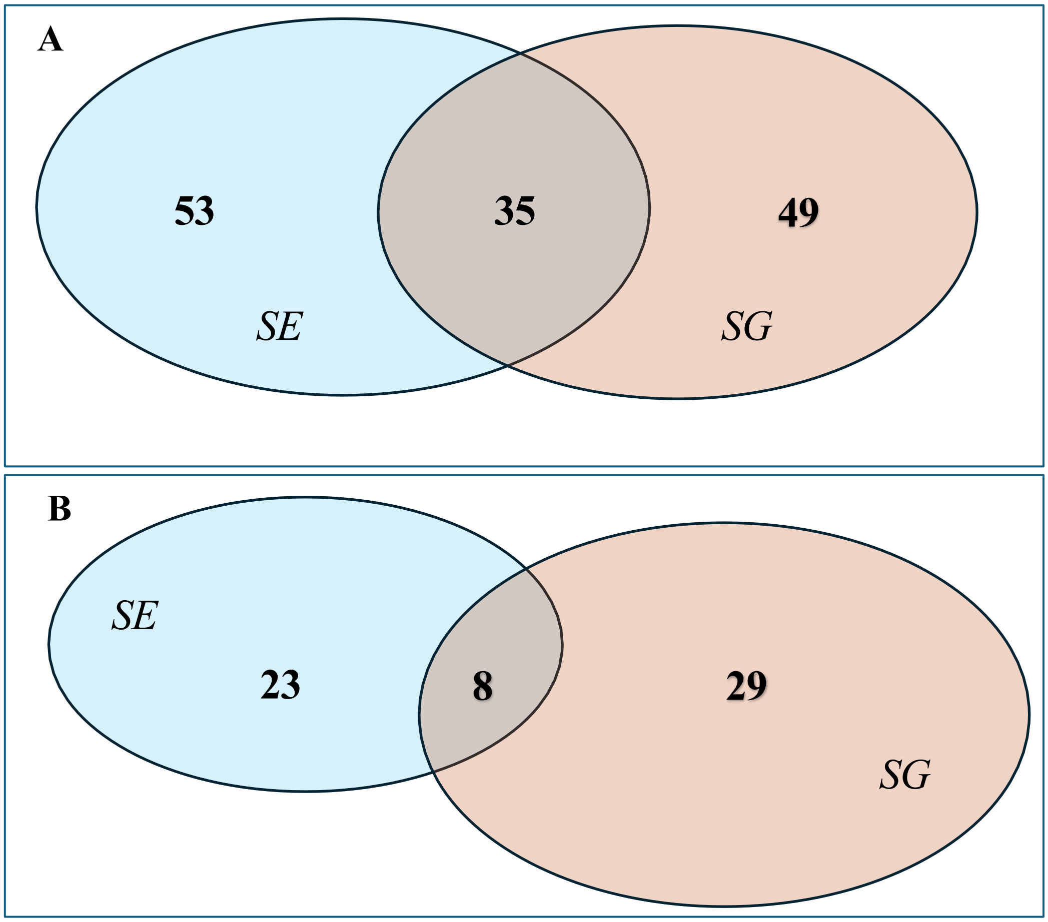

Figure 3.7: Venn diagrams of top 25 genes and GOIs in SE and SG.

(A) Venn diagram illustrating the unique and common genes among the top 25 genes in SE and SG, whether upregulated or downregulated, highly expressed or most changed. ***(B)*** Venn diagram displaying the unique and common GOIs identified from analysis of SE and SG top 25 genes.

After selecting the 60 GOIs, the genes were compiled into an Excel sheet and grouped based on their expression patterns in the WT mouse in the SE, SG, or both. This grouping indicated whether their expression increased or decreased after miR-183 family KO. Similarly, GeneCards was used to manually investigate each gene's function and associated hearing disorders, including hearing loss. Later, this extensive data was divided into two separate tables. The first table displays the gene symbol, the tissue of interest, the change in expression following KO, and the wild-type expression levels in both the SE and SG **(see Table 3.1).**

Table 3.1. Summary of gene expression observations from SE and SG analyses.

Gene Symbol	Tissue	KO Expression ↑ or ↓	KO Expression + and/or Δ	scSE Expression †	scSG Expression ‡
Nnat	SE,SG	↑,↑	+Δ,+Δ	<OHC	E14>P1
Egr1	SE,SG	↑,↑	Δ,Δ	<IHC	E14>P1
Plod2	SE,SG	↑,↑	Δ,+Δ	<HC	E14>P1
Pkp4	SE,SG	↑,↑	+,+	<IHC	E14<P1
Paip2	SE,SG	↑,↑	+,+	=HC	E14<P1
Rims3	SE,SG	↓,↓	+Δ,+Δ	>HC	E14>P1
Ctnna2	SE,SG	↓,↓	Δ,Δ	>IHC	E14>P1
Cntn1	SE,SG	↓,↓	Δ,Δ	<HC	E14<P1
Idh2	SE	↑	+Δ	<HC	
Zfp361l	SE	↑	+	<HC	
Sdc2	SE	↑	+	<HC	
Bace2	SE	↑	Δ	<HC	
Anp32b	SE	↑	+	>HC	
Cfl1	SE	↑	+	>HC	
Dap	SE	↑	+	>HC	
Palld	SE	↑	Δ	>HC	
H3f3b	SE	↑	+	=HC	
Hspa2	SE	↑	Δ	=HC	
Kif5a	SE	↓	+Δ	>HC	
Rnf157	SE	↓	+Δ	>HC	
Gramd1b	SE	↓	+	>HC	
Myo5b	SE	↓	+	>HC	
Prepl	SE	↓	+	>HC	
Amph	SE	↓	Δ	>HC	
Cep85l	SE	↓	Δ	>HC	
Tsc22d3	SE	↓	+Δ	<HC	
Mbnl2	SE	↓	+	<HC	
Rabgap1l	SE	↓	+	<HC	
Trim2	SE	↓	+	<HC	
Map1b	SE	↓	+Δ	=HC	
Mapk8ip1	SE	↓	+	=HC	
Btg1	SG	↑	+		E14>P1
Ccnd3	SG	↑	+		E14>P1
Slc44a2	SG	↑	+		E14>P1
Ttyh3	SG	↑	+		E14>P1
Chd2	SG	↑	Δ		E14>P1
Crebrf	SG	↑	Δ		E14>P1
Kdm6a	SG	↑	Δ		E14>P1
Zbtb20	SG	↑	Δ		E14>P1
Frmd6	SG	↑	Δ		E14>P1
Plag1	SG	↑	Δ		E14>P1

Tmbim6	SG	↑	+	E14<P1
Pdia4	SG	↑	+	E14<P1
Pik3r1	SG	↑	+	E14<P1
Rcn2	SG	↑	+	E14<P1
Prkce	SG	↑	Δ	E14<P1
Rnf208	SG	↑	Δ	E14<P1
Sh3bp4	SG	↑	Δ	E14<P1
Amotl2	SG	↑	Δ	E14<P1
Rps6ka3	SG	↓	+Δ	E14<P1
Tle4	SG	↓	+Δ	E14<P1
Tspan4	SG	↓	+Δ	E14<P1
Sncb	SG	↓	+	E14<P1
Tmod2	SG	↓	+	E14<P1
Maf	SG	↓	+	E14<P1
Brinp2	SG	↓	Δ	E14<P1
Adam23	SG	↓	Δ	E14<P1
Pura	SG	↓	Δ	E14<P1
Dcx	SG	↓	+Δ	E14>P1
Ccdc88a	SG	↓	+	E14>P1

↑ = Increased

↓ = Decreased

+ = Most highly expressed

Δ = Most changed

> = More expressed

< = Less expressed

† Denotes gene changes in expression in the publicly available single-cell RNA seq dataset of P1 WT mouse in the SE (gEAR)

‡ Denotes gene changes in expression in the publicly available single-cell data of embryonic mouse in the SG (gEAR)

= Denotes expression is similar in HCs and OCTs

The second table displays gene symbols, tissues, gene functions, possible hearing disorders, and references related to their role in the inner ear or hearing loss diseases. After examining the current literature on these 60 GOIs for their potential involvement in inner ear development and hearing loss conditions, the following associated genes were identified: *Nnat, Egr1, Plod2, Rims3, Cntn1, Idh2, Cfl1, Palld, H3f3b, Kif5a, Rabgap1l, Map1b, Slc44a2, Zbtb20, Plag1, Prkce, Sncb, Maf,* and *Dcx*. These genes have been previously investigated for their roles, whether partial or complete, in inner ear development, maintenance, or hearing loss-related conditions **(see Table 3.2).**

Table 3.2. Function of GOIs and associated hearing disorders in SE and SG.

Gene symbol	Tissue	Function	Potential Hearing Disorders	Involvement in diseases related to the inner ear or hearing loss
Nnat	SE,SG	Regulation of ion channels during brain development. May also play a role in forming and maintaining the structure of the nervous system	*None	(Wijnholds, 1995) "In addition, expression is observed in the early Rathke's pouch, the derived adenohypophysis, and **the developing inner ear**. During later embryogenesis, the neuronatin gene is **strongly expressed in the major part of the central and peripheral nervous system"**
Egr1	SE,SG	The protein encoded by this gene belongs to the EGR family of C2H2-type zinc-finger proteins. It is a nuclear protein and functions as a transcriptional regulator.	None	(Wang, M., 2021) "These results characterized the expression of EGR-1 in A1 in response to the acoustic input and **suggested the involvement of EGR-1 in auditory function formation**."
Plod2	SE,SG	The protein encoded by this gene is a membrane-bound homodimeric enzyme that is localized to the cisternae of the rough endoplasmic reticulum.	*None/Other Bruck Syndrome (association of osteogenesis imperfecta **"presence of hearing loss"** and congenital joint contractures)	

Pkp4	SE,SG	Involved in regulating junctional plaque organization and cadherin function	None	
Paip2	SE,SG	Enables translation repressor activity. Involved in negative regulation of translational initiation. Located in cytoplasm	None	
Rims3	SE,SG	Predicted to be involved in calcium ion-regulated exocytosis of neurotransmitter	**Heimler syndrome** is a rare autosomal recessive disorder characterized by **sensorineural hearing loss**, enamel hypoplasia of the secondary dentition, and nail abnormalities	
Ctnna2	SE,SG	Enables actin filament binding activity; regulation of neuron migration; and regulation of neuron projection development	None	
Cntn1	SE,SG	Glycosylphosphatidylinositol (GPI)-anchored neuronal membrane protein that functions as a cell adhesion molecule. It may play a role in the formation of axon connections in the developing nervous system	None	(Otzan, 2023) "In the Turkish population, sensitivity to noise-induced hearing loss was observed in five out of eight SNP regions of the TAOK1, TMTC4, NTF3, and CNTN1 genes, with TAOK1, TMTC4, **and CNTN1 genes also being associated with hearing loss"**

Idh2	SE	The protein encoded by this gene is the NADP(+)-dependent isocitrate dehydrogenase found in the mitochondria. It plays a role in intermediary metabolism and energy production	None	(Kim, Y. 2019) "Idh2 deficiency leads to damages to hair cells and spiral ganglion neurons (SGNs) in the cochlea and ultimately to apoptotic cell death and progressive sensorineural hearing loss in Idh2−/− mice. In the present study, we identified that **Idh2 is indispensable for the functional maintenance and survival of hair cells and SGNs."**
Zfp36l1	SE	The encoded protein contains a distinguishing putative zinc finger domain with a repeating cys-his motif. This putative nuclear transcription factor most likely functions in regulating the response to growth factors	None	
Sdc2	SE	Functions as an integral membrane protein and participates in cell proliferation, cell migration and cell-matrix interactions via its receptor for extracellular matrix proteins	None	
Bace2	SE	This gene encodes an integral membrane glycoprotein that functions as an aspartic protease.	None	
Anp32b	SE	Enables RNA polymerase binding activity and histone	None	

		binding activity. Involved in several processes, including activation of cysteine-type endopeptidase activity involved in apoptotic process; nucleosome assembly; and positive regulation of protein export from nucleus		
Cfl1	SE	Cofilin is a widely distributed intracellular actin-modulating protein that binds and depolymerizes filamentous F-actin and inhibits the polymerization of monomeric G-actin in a pH-dependent manner. It is involved in the translocation of actin-cofilin complex from cytoplasm to nucleus	None	(McGrath, 2021) "We also found that loss of the F-actin severing proteins ADF (Actin-Depolymerizing Factor) and cofilin-1 decreased barbed end availability at stereocilia tips… Finally, **stereocilia lengths and widths were dysregulated in Adf and Cfl1 mutants**."
Dap	SE	This gene encodes a basic, proline-rich, 15-kD protein. The protein acts as a positive mediator of programmed cell death that is induced by interferon-gamma	None	
Palld	SE	This gene encodes a cytoskeletal protein that is **required for organizing the**	None	(Park, 2023)

		actin cytoskeleton. The protein is a component of **actin-containing microfilaments**, and it is involved in the control of cell shape, adhesion, and contraction.		"Inner ear hair cells develop mechanosensitive hair bundles on their apical surface to convert sounds and accelerations into electrical signals. Each hair bundle consists of about 100 stereocilia arranged in rows of increasing height and width; this precise structure is essential for mechanoelectrical transduction (MET). The **actin cytoskeleton** plays a crucial role in establishing this architecture."
H3f3b	SE	Histones are basic nuclear proteins responsible for the nucleosome structure of the chromosomal fiber in eukaryotes. Two molecules of each of the four core histones (H2A, H2B, H3, and H4) form an octamer, around which approximately 146 bp of DNA is wrapped in repeating units, called nucleosomes.	None/Other Bryant-Li-Bhoj Neurodevelopmental Syndrome 2 (Additional features may include **hearing loss**, seizures, short stature, and mild skeletal defects)	
Hspa2	SE	Enables disordered domain-specific binding activity; enzyme binding activity; and unfolded protein binding activity.	None	
Kif5a	SE	This gene encodes a member of the Kinesin protein family. Members of this	None	(Muglia, 2014)

		family are part of a multisubunit complex that functions as a microtubule motor in intracellular organelle transport.		"We identified a novel mutation in the *KIF5A* gene in two siblings affected by paraparesis **associated with deafness**. So far, about 20 mutations have been reported in the *KIF5A* gene and most of them are located in the highly conserved kinesin motor domain, which plays an important **role in the interaction with the neuronal microtubular system**."
Rnf157	SE	Predicted to be involved in several processes, including negative regulation of signal transduction; positive regulation of dendrite extension; and protein autoubiquitination.	None	
Gramd1b	SE	Predicted to enable cholesterol binding activity; cholesterol transfer activity; and phospholipid binding activity	None	
Myo5b	SE	The protein encoded by this gene, together with other proteins, may be involved in plasma membrane recycling.	None	
Prepl	SE	The protein encoded by this gene belongs to the prolyl oligopeptidase subfamily of	None	

		serine peptidases. Mutations in this gene have been associated with hypotonia-cystinuria syndrome		
Amph	SE	This gene encodes a protein associated with the cytoplasmic surface of synaptic vesicles.	None	
Cep85l	SE	The protein encoded by this gene was identified as a breast cancer antigen. Nothing more is known of its function currently	None	
Tsc22d3	SE	This gene encodes the anti-inflammatory protein glucocorticoid (GC)-induced leucine zipper.	None	
Mbnl2	SE	This gene is a member of the muscleblind protein family which was initially described in Drosophila melanogaster. This gene encodes a C3H-type zinc finger protein that modulates alternative splicing of pre-mRNAs	None	
Rabgap1l	SE	Enables GTPase activator activity and small GTPase binding activity. Acts upstream of or within the regulation of protein localization. Located in the Golgi apparatus; early endosome; and nucleus	Cholesteatoma Of Middle Ear **Hearing loss**, dizziness, and facial muscle paralysis are rare but can result from continued Cholesteatoma growth	
Trim2	SE	The protein localizes to cytoplasmic filaments. It plays a neuroprotective role and functions as an E3-	None	

		ubiquitin ligase in proteasome-mediated degradation of target proteins		
Map1b	SE	This gene encodes a protein that belongs to the microtubule-associated protein family. The proteins of this family are thought to be involved in microtubule assembly, which is an essential step in neurogenesis.	**Deafness, Autosomal Dominant 83**/ Autosomal dominant deafness-83 (DFNA83) is characterized by **the onset of progressive sensorineural hearing loss** at an average age of 24 years. A notable finding is a normal distortion product otoacoustic emissions (DPOAE) test, implicating dysfunction of spiral ganglia neurons rather than outer hair cells as a disease mechanism	(Cui, 2020) "Map1b deficiency yielded defects in the morphology and electrophysiology of spiral ganglion neurons, but it did not affect the morphologies of the cochlea in mice. Therefore, **our data demonstrate that dysfunctions of spiral ganglion neurons induced by MAP1B deficiency caused hearing loss**."
Mapk8ip1	SE	This protein has been shown to prevent MAPK8-mediated activation of transcription factors and to decrease IL-1 beta and MAP kinase kinase 1 (MEKK1) induced apoptosis in pancreatic beta cells	None	
Btg1	SG	This gene is a member of an anti-proliferative gene family that regulates cell growth and differentiation.	None	

Ccnd3	SG	This cyclin forms a complex with and functions as a regulatory subunit of CDK4 or CDK6, whose activtiy is required for cell cycle G1/S transition. This protein has been shown to interact with and be involved in the phosphorylation of tumor suppressor protein Rb.	None	
Slc44a2	SG	Enables choline transmembrane transporter activity. Involved in choline transport and transmembrane transport. Located in mitochondrion and plasma membrane	None	(Koehl, 2023) "Interestingly, **the first-ever reported SLC44A2-deficient individuals suffer from progressive hearing impairment**, recurrent arterial aneurysms, and epilepsy."; "Moreover**, knockout of the Slc44a2 gene also caused hair cell and spiral ganglion neuron loss, especially in the basal turn of the cochlea**, and Slc44a2 null mice exhibited high-frequency hearing loss."
Ttyh3	SG	The protein encoded by this gene is a membrane-bound homodimeric enzyme that is localized to the cisternae of the rough endoplasmic reticulum. The enzyme catalyzes the hydroxylation of lysyl residues in collagen-like peptides.	None	
Chd2	SG	CHD genes alter gene expression possibly by modification of chromatin structure thus altering access of the transcriptional	None	

		apparatus to its chromosomal DNA template.		
Crebrf	SG	Involved in negative regulation of endoplasmic reticulum unfolded protein response; positive regulation of transport; and regulation of transcription by RNA polymerase II.	None	
Kdm6a	SG	This gene is located on the X chromosome and is the corresponding locus to a Y-linked gene which encodes a tetratricopeptide repeat (TPR) protein	None	
Zbtb20	SG	This gene acts as a transcriptional repressor and plays a role in neurogenesis, glucose homeostasis, and postnatal growth.	None	(Xie, 2023) "Here, we show that the zinc-finger protein ZBTB20 is required for cochlear maturation and hearing. **Deletion of Zbtb20 specifically in the cochlear epithelium causes profound deafness with reduced endolymph potential in mice**… This study establishes the essential role of ZBTB20 in cochlear maturation and hearing."
Frmd6	SG	Predicted to be involved in actomyosin structure organization; Act upstream of or within apical constriction; cellular protein localization; and regulation	None	

		of actin filament-based process.		
Plag1	SG	Pleomorphic adenoma gene 1 encodes a zinc finger protein with 2 putative nuclear localization signals.	None	(Tran, 2021) "The cued test of fear conditioning, prepulse inhibition of the startle response, and Preyer's reflex test suggest that **Plag1 KO mice may have a hearing impairment**. **This implies that PLAG1 plays an important role in proper functioning and/or development of the neural circuitry behind the auditory processes** or interacts with genes involved in those processes."
Tmbim6	SG	Involved in negative regulation of RNA metabolic process and negative regulation of intrinsic apoptotic signaling pathway. Acts upstream of or within negative regulation of calcium ion transport into the cytosol.	None	
Pdia4	SG	This gene encodes a member of the disulfide isomerase family of ER proteins that catalyze protein folding and thiol-disulfide interchange reactions.	None	
Pik3r1	SG	Phosphatidylinositol 3-kinase plays an important role in the metabolic actions of insulin, and a mutation in this gene has been associated with insulin resistance.	None	

Rcn2	SG	The protein encoded by this gene is a calcium-binding protein located in the lumen of the ER. The protein contains six conserved regions with similarity to a high-affinity Ca(+2)-binding motif.	None	
Prkce	SG	Family of serine- and threonine-specific protein kinases that can be activated by calcium and the second messenger diacylglycerol. They phosphorylate a wide variety of protein targets and are known to be involved in diverse cellular signaling pathways.	None/Other Short Syndrome (Other signs and symptoms that have been reported in people with SHORT syndrome include immune system abnormalities, a kidney disorder known as nephrocalcinosis**, hearing loss…**	(Li, 2021) “SNPs (Single Nucleotide Polymorphism) antioxidant genes are also involved in hearing loss by influencing Nrf2. PRKCE and TGF-β1 are two members of Nrf2 signaling pathway. **Three SNPs of the PRKCE gene** and two SNPs of the TGF-β1 gene are closely **related to ARHL (age-related hearing loss)** in a matched and control study of healthy volunteers and elderly deafness patients.”
Rnf208	SG	Enables ubiquitin-protein transferase activity. Involved in protein autoubiquitination. Located in cytosol and nucleoplasm.	None	
Sh3bp4	SG	This protein is involved in cargo-specific control of clathrin-mediated endocytosis, specifically controlling the	None	

		internalization of a specific protein receptor		
Amotl2	SG	Angiomotin is a protein that binds angiostatin, a circulating inhibitor of the formation of new blood vessels (angiogenesis). Angiomotin mediates angiostatin inhibition of endothelial cell migration and tube formation in vitro.	None	
Rps6ka3	SG	This kinase contains 2 non-identical kinase catalytic domains and phosphorylates various substrates, including members of the mitogen-activated kinase (MAPK) signaling pathway. The activity of this protein has been implicated in controlling cell growth and differentiation.	None	
Tle4	SG	Predicted to enable transcription corepressor activity. Predicted to be involved in negative regulation of canonical Wnt signaling pathway.	None	
Tspan4	SG	The proteins mediate signal transduction events that play a role in the regulation of cell development, activation, growth and motility.	None	
Sncb	SG	This gene encodes a member of a small family of proteins that inhibit phospholipase D2 and may function in neuronal plasticity.	None	(Akil, 2008) "Together, these results localize synucleins to the efferent cholinergic

				neuronal auditory system, **pointing to a role in normal auditory function, and raising the potential implications for their role in auditory neurodegenerative disorders.**”
Tmod2	SG	This gene encodes a neuronal-specific member of the tropomodulin family of actin-regulatory proteins. The encoded protein caps the pointed end of actin filaments preventing both elongation and depolymerization.	None	
Maf	SG	This protein plays a role in the regulation of several cellular processes, including embryonic lens fiber cell development, increased T-cell susceptibility to apoptosis, and chondrocyte terminal differentiation.	None/Other Ayme-Gripp Syndrome (Signs and symptoms can vary and may include brachycephaly or plagiocephaly; structural brain abnormalities; abnormal EEG; intellectual disability; and **deafness**)	
Brinp2	SG	Predicted to be involved in the cellular response to retinoic acid; negative regulation of mitotic cell cycle; and positive regulation of neuron differentiation. Predicted to	None	

		be active in dendrites; endoplasmic reticulum; and neuronal cell body.		
Adam23	SG	This gene encodes a member of the ADAM (a disintegrin and metalloprotease domain) family. Implicated in a variety of biological processes involving cell-cell and cell-matrix interactions, including fertilization, muscle development, and neurogenesis.	None	
Pura	SG	Single-stranded DNA-binding protein. It binds preferentially to the single strand of the purine-rich element termed PUR, which is present at origins of replication and in gene flanking regions in a variety of eukaryotes from yeasts through humans. Implicated in the control of both DNA replication and transcription.	None	
Dcx	SG	The encoded protein appears to direct neuronal migration by regulating the organization and stability of microtubules. Mutations in this gene cause abnormal migration of neurons during	None	(Freemyer, 2019) “Auditory brainstem response was used to measure **hearing loss**. Unilateral hearing loss was evident in all sound damaged

		development and disrupt the layering of the cortex.		animals. **Hearing loss related decreases in DCX** expression were evident bilaterally in the DG (hippocampal dentate gyrus) while hearing loss related increases in DCX expression were evident bilaterally in the PFL (cerebellar parafloccular lobe)
Ccdc88a	SG	The encoded protein is an actin-binding protein that is activated by the serine/threonine kinase Akt and plays a role in cytoskeleton remodeling and cell migration.	None	

* None = No hearing disorders directly linked to the gene

* None/Other = No gene-related hearing disorder, but deafness or hearing loss occurs as a symptom of a different condition

Further analysis using Gene Ontology (GO) with DAVID (the Database for Annotation, Visualization, and Integrated Discovery) validated the cellular components (CC), molecular functions (MF), and biological processes (BP) associated with these 60 GOIs. **Tables 3.3 and 3.4** display the GO term analysis for the SE and SG, respectively.

Table 3.3. Gene ontology enrichment analysis of 37 genes in SE.

Sensory Epithelia			
GOTERM Cellular Component (GOTERM_CC_DIRECT)			
Cellular Component	Count	Genes	P Values
Cytoplasm	21	EGR1, MBNL2, TSC22D3, CEP85L, HSPA2, ZFP36L1, MAPK8IP1, RNF157, PREPL, PALLD, MAP1B, TRIM2, MYO5B, CFL1, KIF5A, NNAT, PKP4, AMPH, CTNNA2, ANP32B, PAIP2	1.75E-04
Neuronal cell body	7	PALLD, SDC2, MAP1B, MYO5B, CFL1, KIF5A, MAPK8IP1	2.26E-04
Cytoskeleton	9	PREPL, PALLD, MAP1B, CEP85L, CFL1, PKP4, AMPH, CTNNA2, HSPA2	4.90E-04
Axon	6	PALLD, MAP1B, KIF5A, CNTN1, CTNNA2, MAPK8IP1	5.92E-04
Actin cytoskeleton	4	PALLD, MYO5B, CFL1, CTNNA2	0.005015958
Perinuclear region of cytoplasm	5	MAP1B, MYO5B, KIF5A, PKP4, MAPK8IP1	0.027959481
Growth cone	3	PALLD, MAP1B, CFL1	0.029149243
Lamellipodium	3	PALLD, CFL1, CTNNA2	0.032240769
Dendritic spine	3	MAP1B, MYO5B, CFL1	0.034272983
Cell-cell junction	3	CFL1, PKP4, CTNNA2	0.038792002
Apical dendrite	2	MAP1B, KIF5A	0.041658595
Glutamatergic synapse	4	RIMS3, MYO5B, CFL1, AMPH	0.060817499
Axonal growth cone	2	PALLD, MAPK8IP1	0.063786987
Postsynaptic density	3	MAP1B, PKP4, CTNNA2	0.066296249
Nucleus	14	EGR1, RABGAP1L, MBNL2, H3F3B, TSC22D3, HSPA2, ZFP36L1, MAPK8IP1, PREPL, PALLD, CFL1, PKP4, CTNNA2, ANP32B	0.074429059
Anchoring Junction	3	PALLD, PKP4, CTNNA2	0.097673309

GOTERM Molecular Function (GOTERM_MF_DIRECT)			
Actin binding	4	PALLD, MAP1B, MYO5B, CFL1	0.020247021
Translation repressor activity	2	TRIM2, PAIP2	0.029501801
RNA polymerase II core promoter sequence-specific DNA binding	2	EGR1, H3F3B	0.036745064
Protein binding	14	SDC2, TSC22D3, HSPA2, ZFP36L1, MAPK8IP1, RNF157, PREPL, MAP1B, TRIM2, MYO5B, CFL1, KIF5A, CNTN1, AMPH	0.040245298
Actin filament binding	3	MYO5B, CFL1, CTNNA2	0.04463675
Small GTPase binding	3	RABGAP1L, RIMS3, MYO5B	0.074055617
Kinesin binding	2	KIF5A, MAPK8IP1	0.079122216
Cadherin binding	2	PKP4, CTNNA2	0.098277461
GOTERM Biological Process (GOTERM_BB_DIRECT)			
Regulation of protein localization	3	RABGAP1L, MYO5B, NNAT	0.01197875
Modification of postsynaptic actin cytoskeleton	2	CFL1, CTNNA2	0.01768257
Regulation of translation	3	DAP, PAIP2, ZFP36L1	0.02237927
Cellular response to peptide hormone stimulus	2	MAP1B, ZFP36L1	0.02930262
Cell-cell adhesion	3	CNTN1, PKP4, CTNNA2	0.04035573
Regulation of neuron apoptotic process	2	EGR1, TRIM2	0.04648393
Vesicle-mediated transport	3	MYO5B, KIF5A, MAPK8IP1	0.05440612
Cell migration	3	PALLD, SDC2, CTNNA2	0.06581771
Regulation of synaptic vesicle exocytosis	2	PREPL, RIMS3	0.06615736
Positive regulation of axon extension	2	MAP1B, MYO5B	0.06615736
Dendrite morphogenesis	2	SDC2, CTNNA2	0.07170588

Table 3.4. Gene ontology enrichment analysis of 31 genes in SG.

Spiral Ganglion			
GOTERM Cellular Component (GOTERM_CC_DIRECT)			
Term	Count	Genes	P Values
Cytoplasm	23	EGR1, BTG1, PRKCE, TMOD2, ZBTB20, PIK3R1, CCDC88A, PURA, RPS6KA3, BRINP2, CCND3, MAF, FRMD6, NNAT, CREBRF, DCX, SH3BP4, PKP4, TMBIM6, AMOTL2, CTNNA2, SNCB, PAIP2	0.00107056
Presynaptic membrane	3	RIMS3, ADAM23, CNTN1	0.04100465
Growth cone	3	TMOD2, DCX, SNCB	0.04338214
Presynaptic cytosol	2	PRKCE, SNCB	0.053076
Nucleus	17	TLE4, EGR1, BTG1, PLAG1, PRKCE, ZBTB20, PIK3R1, CHD2, PURA, RPS6KA3, CCND3, MAF, CREBRF, SH3BP4, PKP4, CTNNA2, KDM6A	0.05501367
Cell-cell junction	3	PKP4, CTNNA2, PIK3R1	0.05733298
Cytoskeleton	6	CCDC88A, FRMD6, PRKCE, TMOD2, PKP4, CTNNA2	0.09108394
Postsynaptic density	3	PURA, PKP4, CTNNA2	0.09636664
GOTERM Molecular Function (GOTERM_MF_DIRECT)			
Protein binding	18	TLE4, SLC44A2, PRKCE, PIK3R1, CHD2, CCDC88A, PURA, RPS6KA3, CCND3, MAF, RCN2, FRMD6, ADAM23, CNTN1, DCX, TSPAN4, AMOTL2, KDM6A	0.00855332
Protein kinase binding	5	RPS6KA3, CCND3, PRKCE, DCX, PIK3R1	0.01957012
Translation repressor activity, nucleic acid binding	2	PURA, PAIP2	0.02335799
GDP-dissociation inhibitor activity	2	CCDC88A, SH3BP4	0.02690419
Double-stranded DNA binding	3	EGR1, PURA, MAF	0.03925128
Insulin receptor binding	2	CCDC88A, PIK3R1	0.04792045

RNA polymerase II core promoter proximal region sequence-specific DNA binding	6	EGR1, MAF, PLAG1, ZBTB20, CHD2, KDM6A	0.05008937
Transcriptional activator activity, RNA polymerase II transcription regulatory region sequence-specific binding	4	EGR1, MAF, PLAG1, CREBRF	0.07679252
GOTERM Biological Process (GOTERM_BB_DIRECT)			
Response to endoplasmic reticulum stress	4	CREBRF, TMBIM6, PIK3R1, PDIA4	7.49E-04
Positive regulation of gene expression	6	EGR1, MAF, PLAG1, CNTN1, PIK3R1, KDM6A	0.00340732
Negative regulation of transcription from RNA polymerase II promoter	7	TLE4, EGR1, PURA, CCND3, MAF, CREBRF, ZBTB20	0.00853298
Negative regulation of hypoxia-induced intrinsic apoptotic signaling pathway	2	TMBIM6, KDM6A	0.01549023
Positive regulation of transcription from RNA polymerase II promoter	7	EGR1, RPS6KA3, MAF, PLAG1, CREBRF, PIK3R1, KDM6A	0.01991583
Cell adhesion	5	PRKCE, ADAM23, CNTN1, PKP4, CTNNA2	0.02201538
Nervous system development	4	PURA, CCDC88A, BRINP2, DCX	0.03837019
Cell-cell adhesion	3	CNTN1, PKP4, CTNNA2	0.05333499
Negative regulation of mitotic cell cycle	2	BRINP2, BTG1	0.05402492
Brain development	3	NNAT, CNTN1, DCX	0.05825904
Regulation of neuron projection development	2	CCDC88A, CTNNA2	0.07193265
Positive regulation of cytokinesis	2	PRKCE, PKP4	0.07515303
Dendrite morphogenesis	2	DCX, CTNNA2	0.08315655
Positive regulation of myoblast differentiation	2	BTG1, PIK3R1	0.08951089
Insulin secretion	2	PRKCE, NNAT	0.08951089
Response to unfolded protein	2	CREBRF, TMBIM6	0.09267199

To refine the list of 60 GOIs, gene selection focused on genes showing expression changes after miR-183 family KO, either upregulated (expected) or downregulated (indirect). The functions of these genes and their connections to hearing disorders were also examined. This process resulted in the identification of 19 GOIs. In the SE, *Egr1* (Early Growth Response 1), *Nnat* (Neuronatin), and *Plod2* (Procollagen-Lysine, 2-Oxoglutarate 5-Dioxygenase 2) were selected because they were expressed in both the SE and SG and showed increased expression after KO, aligning with expectations. *Rims3* (Regulating Synaptic Membrane Exocytosis Protein 3) and *Cntn1* (Contactin 1), also present in both tissues, decreased after knockout, suggesting an indirect effect. Conversely, *Idh2* (Isocitrate Dehydrogenase (NADP (+)) 2), *Cfl1* (Cofilin 1), *Anp32b* (Acidic Nuclear Phosphoprotein 32 Family), *Palld* (Palladin, Cytoskeletal-Associated Protein), and *Hspa2* (Heat Shock Protein Family A (Hsp70) Member 2) were expressed only in the SE and increased after knockout, as anticipated. Similarly, *Kif5a* (Kinesin Family Member 5A) and *Map1b* (Microtubule-Associated Protein 1B) were exclusive to the SE but decreased after knockout, hinting at an indirect effect. In the SG, *Zbtb20* (Zinc Finger and BTB Domain Containing 20), *Plag1* (Pleiomorphic Adenoma Gene 1 Protein), *Prkce* (Protein Kinase C Epsilon), *Amotl2* (Angiomotin-Like 2), and *Slc44a2* (Solute Carrier Family 44 Member 2) were upregulated following knockout. Conversely, *Dcx* (Doublecortin) and *Sncb* (Synuclein Beta) were downregulated. A comprehensive analysis, including knockout effects, gene functions, and association with hearing loss or inner ear development, and Gene Ontology (GO) analysis, narrowed the list from 19 to 9 GOIs: *Egr1, Nnat, Plod 2, Rims3, Kif5a, Idh2, Zbtb20, Slc44a2*, and *Sncb*. Four genes—*Egr1, Nnat, Plod 2,* and *Rims3*—stand out as promising for future validation via immunostaining, supported by existing literature as detailed in **Table 3.5.**

Although there is no reported literature on Rims3, it remains an interesting gene to validate, as an antibody is available from *Abcam* for immunostaining.

Table 3.5. Selection of antibodies for Egr1, Nnat, Plod2, and Rims3 in the SE and SG.

Gene Symbol	KO Expression		scSE Expression †	scSG Expression ‡	Function	Reference
Egr1	↑,↑	Δ,Δ	<IHC	E14>P1	Nuclear protein that functions as a transcriptional regulator. Also involved in auditory function formation.	Mouse ab300449 (abcam) (Kanemaru, 2021)
Nnat	↑,↑	+Δ,+Δ	<OHC	E14>P1	Regulates ion channels during brain development and plays a role in forming and maintaining the nervous system's structure. Also expressed in the developing inner ear.	Mouse ab27266 (abcam) (Vatsa, 2019)
Plod2	↑,↑	Δ,+Δ	<HC	E14>P1	Membrane-bound homodimeric enzyme in the rough ER. Involved in a genetic defect that is associated with the presence of hearing loss.	Mouse ab313765 (abcam) (Yin, 2025)
Rims3	↓,↓	+Δ,+Δ	>HC	E14>P1	Predicted to be involved in calcium-ion regulation. It is involved in Heimler Syndrome, an autosomal recessive disorder with sensorineural hearing loss.	Mouse ab192602 (abcam)

Chapter 4: Discussion

Hearing loss is a significant and growing global health issue, impacting people across all ages and hitting low- and middle-income countries hardest. In 2021, the World Health Organization projected that nearly 1 in 4 people worldwide—approximately 2.5 billion—will experience some form of hearing impairment by 2050. This makes hearing loss a critical area in biomedical research, bridging basic science, clinical innovation, and public health efforts, with ongoing advancements offering hope to transform lives. Hearing loss can be caused by various factors such as ototoxic drugs, noise exposure, and genetic damage to auditory cells like hair cells (HCs) and spiral ganglion neurons (SGNs). Unfortunately, unlike other vertebrates, mammals have limited or no capacity to regenerate these hair cells after injury.

Previous research has highlighted the importance of microRNAs in the development and maintenance of hair cells within the inner ear. Studies involving conditional knockout of Dicer demonstrated that Dicer activity is crucial for maintaining healthy, functional hair cells in the cochlear sensory epithelium (Friedman, 2009). Dicer is an essential enzyme for the maturation and proper function of microRNAs. Consequently, removing Dicer from the sensory epithelium leads to abnormal hair cell growth and subsequent degeneration, resulting in deafness (Friedman, 2009). Notably, a deficiency in the miR-183 family causes significant defects in hair cell differentiation, morphogenesis, and function, which causes severe congenital syndromic deafness in mice (Geng, 2018).

Given the importance of the miR-183 family in the development and maintenance of the inner ear, as well as its link to hereditary deafness in both humans and mice, the research team performed bulk RNA sequencing to compare the WT and KO of the miR-183 family. As a result, the expression levels of many genes across all cell types were obtained. Therefore, in this project, the goal was to extract cellular-resolution from existing bulk RNA sequencing data using publicly available scRNA-seq data from gEAR ("P1, mouse, scRNA seq, cochlear epithelium" [Kolla et al. 2020]). It is worth noting that there are other databases and datasets beyond gEAR for achieving cellular-resolution analysis from bulk RNA-seq. Examples include "Insights into the biology of hearing and deafness revealed by single-cell RNA-sequencing" (Ranum et al. 2019) and "Characterization of transcriptomes of cochlear inner and outer hair cells (Liu et al., 2014)." These researchers physically isolated and pooled individual inner hair cells (IHCs), outer hair cells (OHCs), and Deiters' cells (DCs) from the murine cochlea. However, the datasets from Kolla et al. 2020, isolated mouse cochlear cells at different developmental time points, enabling the extraction of cellular-resolution data from hair cells and supporting cells within the bulk RNA-seq dataset to identify GOIs after miR183 KO.

Several heatmaps were generated to visualize and explore cell-specific gene expression patterns in different cochlear cell types and spiral ganglion neurons. These heatmaps were then examined to identify 60 GOIs in both the SE and SG. These 60 GOIs were further analyzed using GeneCards to gather more information about their names, functions, and associated hearing-related disorders. Finally, GO analysis was performed, further narrowing the list to 4 GOIs: Egr1, Nnat, Plod2, and Rims3, gene candidates that could be further validated by immunofluorescence.

A potential limitation of this work is the lack of validation, such as immunostaining of the four GOIs; however, the primary goal was to develop an approach that could provide cellular resolution for approximately 1,616 conserved miR-183 family KO-predicted target genes in the mouse genome. To achieve this, a step-by-step method was implemented to identify a refined list of GOIs that changed in expression after KO. As a result, four specific GOIs were identified from a list of over 1,000 genes.

Unlike bulk RNA-seq, this method provides a practical way to identify specific miR-183 family KO target genes that exhibit a change in expression. However, bulk RNA-seq provided an excellent starting point for the project, as it helps identify differentially expressed genes and is more cost-effective. This dataset was combined with a publicly available scRNA-seq dataset, enabling evaluation of cell-specific expression changes. This approach may be comparable to spatial transcriptomics, which can reveal and analyze differences in gene expression between individual cells and cell types within tissue. It involves preparing and fixing the tissue and determining the sample identities before performing spatial transcriptomics.

Additionally, during the heatmaps analysis, some genes in the top 25 were excluded because they lacked distinctive expression patterns. These genes were not included in the selection of GOIs, but they may be relevant in other contexts and should not be dismissed entirely. Since the main goal was to narrow the extensive gene list, the focus was on identifying patterns of high or low expression, hair cell specificity, and neuronal maturity to address the research question.

Another key point is that, although the total 60 GOIs were further reduced by selecting only a few, the remaining ones remain equally important. Several predicted target genes of the miR-183 family, known for their crucial roles in hair cell (HC) development and function—such as *Clic5, Rdx, Ezr, Rac1, Myo1c, Pvrl3*, and *Sox2*—are upregulated in the cochlea (Geng, 2018). Notably, myosin-1c (*Myo1c*) is essential for hair cell mechanotransduction adaptation. *Cyr et al*. (2002) showed that the neck region of *Myo1c* binds to receptors at stereociliary tips—where transduction occurs—as well as in the pericuticular necklace (a vesicle-rich area around the cuticular plate), the kinocilium (a cilium at the hair bundle's edge), and inside the hair-cell soma. Since Myo1c was mentioned, the 60 GOIs were revised, revealing that *Myo5b*, another myosin, was also upregulated in P1 WT mice and downregulated after P0 miR-KO. But how are *Myo1c* and *Myo5b* connected? Both are myosin. Additionally, *Kaji et al.* (2020) demonstrated that the loss of *Myo5b* increased the expression of several genes, including *Myo5c* and *Myo1c*. Similarly, in this dataset, *Myo5b* expression decreased after miR-183 family KO. This suggests that decreased *Myo5b* might lead to increased *Myo1c* expression, potentially disrupting the regulation of hair cell morphology and mechanotransduction.

While validating these findings using immunofluorescence across the four GOIs is essential, single-nucleus RNA sequencing (snRNA-seq) could also be performed, where nuclei are flash-frozen until all cells are ready for library preparation. Alternatively, spatial transcriptomics might be employed, though it can be more challenging and costly. Overall, these findings could advance the field of hearing research in the biomedical sciences by providing a detailed cellular-level evaluation and pinpointing specific genes affected by miR-183 family knockouts, which are crucial for the development and maintenance of the inner ear.

Chapter 5: References

Akil, O., Weber, C. M., Park, S. N., Ninkina, N., Buchman, V., & Lustig, L. R. (2008). Localization of synucleins in the mammalian cochlea. *Journal of the Association for Research in Otolaryngology : JARO*, *9*(4), 452–463.

Banks, S.A., Pierce, M.L. & Soukup, G.A. (2020). Sensational MicroRNAs: Neurosensory Roles of the MicroRNA-183 Family. *Molecular neurobiology*, *57*(1), 358–371.

Burns, J. C., Kelly, M. C., Hoa, M., Morell, R. J., & Kelley, M. W. (2015). Single-cell RNA-Seq resolves cellular complexity in sensory organs from the neonatal inner ear. *Nature communications*, *6*, 8557.

Cui, L., Zheng, J., Zhao, Q., Chen, J. R., Liu, H., Peng, G., Wu, Y., Chen, C., He, Q., Shi, H., Yin, S., Friedman, R. A., Chen, Y., & Guan, M. X. (2020). Mutations of MAP1B encoding a microtubule-associated phosphoprotein cause sensorineural hearing loss. *JCI insight*, *5*(23), e136046.

Cyr, J. L., Dumont, R. A., & Gillespie, P. G. (2002). Myosin-1c interacts with hair-cell receptors through its calmodulin-binding IQ domains. *The Journal of neuroscience : the official journal of the Society for Neuroscience*, *22*(7), 2487–2495.

Fan, J., Jia, L., Li, Y., Ebrahim, S., May-Simera, H., Wood, A., Morell, R. J., Liu, P., Lei, J., Kachar, B., Belluscio, L., Qian, H., Li, T., Li, W., Wistow, G., & Dong, L. (2017). Maturation arrest in early postnatal sensory receptors by deletion of the miR-183/96/182 cluster in mouse. *Proceedings of the National Academy of Sciences of the United States of America*, *114*(21), E4271–E4280.

Freemyer, A., Neal, C., Nelson-Brantley, J., Staecker, H., & Durham, D. (2019). Early Onset Region and Cell Specific Alterations of Doublecortin Expression in the CNS of Animals with Sound Damage Induced Hearing Loss. *IBRO reports*, *7*, 129–140.

Friedman, L. M., Dror, A. A., Mor, E., Tenne, T., Toren, G., Satoh, T., Biesemeier, D. J., Shomron, N., Fekete, D. M., Hornstein, E., & Avraham, K. B. (2009). MicroRNAs are essential for development and function of inner ear hair cells in vertebrates. Proceedings of the National Academy of Sciences of the United States of America, 106(19), 7915–7920.

Geng, R., Furness, D. N., Muraleedharan, C. K., Zhang, J., Dabdoub, A., Lin, V., & Xu, S. (2018). The microRNA-183/96/182 Cluster is Essential for Stereociliary Bundle Formation and Function of Cochlear Sensory Hair Cells. *Scientific reports*, *8*(1), 18022.

Huang, daW., Sherman, B. T., & Lempicki, R. A. (2009). Systematic and integrative analysis of large gene lists using DAVID bioinformatics resources. *Nature protocols*, *4*(1), 44–57.

Jin, Z. B., Hirokawa, G., Gui, L., Takahashi, R., Osakada, F., Hiura, Y., Takahashi, M., Yasuhara, O., & Iwai, N. (2009). Targeted deletion of miR-182, an abundant retinal microRNA. *Molecular vision, 15*, 523–533.

Kaji, I., Roland, J. T., Watanabe, M., Engevik, A. C., Goldstein, A. E., Hodges, C. A., & Goldenring, J. R. (2020). Lysophosphatidic Acid Increases Maturation of Brush Borders and SGLT1 Activity in MYO5B-deficient Mice, a Model of Microvillus Inclusion Disease. Gastroenterology, 159(4), 1390–1405.e20.

Kanemaru, H., Mizukami, Y., Kaneko, A., Tagawa, H., Kimura, T., Kuriyama, H., Sawamura, S., Kajihara, I., Makino, K., Miyashita, A., Aoi, J., Makino, T., Masuguchi, S., Fukushima, S., & Ihn, H. (2021). A mechanism of cooling hot tumors: Lactate attenuates inflammation in dendritic cells. *iScience*, *24*(9), 103067.

Kim, C. W., Han, J. H., Wu, L., & Choi, J. Y. (2018). microRNA-183 is Essential for Hair Cell Regeneration after Neomycin Injury in Zebrafish. *Yonsei medical journal*, *59*(1), 141–147.

Kim, Y. R., Baek, J. I., Kim, S. H., Kim, M. A., Lee, B., Ryu, N., Kim, K. H., Choi, D. G., Kim, H. M., Murphy, M. P., Macpherson, G., Choo, Y. S., Bok, J., Lee, K. Y., Park, J. W., & Kim, U. K. (2019). Therapeutic potential of the mitochondria-targeted antioxidant MitoQ in mitochondrial-ROS induced sensorineural hearing loss caused by Idh2 deficiency. *Redox biology*, *20*, 544–555.

Koehl, B., Vrignaud, C., Mikdar, M., Nair, T. S., Yang, L., Landry, S., Laiguillon, G., Giroux-Lathuile, C., Anselme-Martin, S., El Kenz, H., Hermine, O., Mohandas, N., Cartron, J. P., Colin, Y., Detante, O., Marlu, R., Le Van Kim, C., Carey, T. E., Azouzi, S., & Peyrard, T. (2023). Lack of the human choline transporter-like protein SLC44A2 causes hearing impairment and a rare red blood phenotype. *EMBO molecular medicine*, *15*(3), e16320.

Kolla, L., Kelly, M. C., Mann, Z. F., Anaya-Rocha, A., Ellis, K., Lemons, A., Palermo, A. T., So, K. S., Mays, J. C., Orvis, J., Burns, J. C., Hertzano, R., Driver, E. C., & Kelley, M. W. (2020). Characterization of the development of the mouse cochlear epithelium at the single-cell level. *Nature communications*, *11*(1), 2389.

Lavoro, A., Gattuso, G., Grillo, C.M., Spandidos, D.A., Salmeri, M., Lombardo, C......Falzone, L. (2022). Role of microRNAs as novel diagnostic biomarkers and potential therapeutic targets for hearing disorders (Review). *International Journal of Epigenetics*, 2, 3.

Lewis, M. A., Lachgar-Ruiz, M., Di Domenico, F., Duddy, G., Chen, J., Fernandez, S., Morin, M., Williams, G., Moreno Pelayo, M. A., & Steel, K. P. (2024). Pathological mechanisms and candidate therapeutic approaches in the hearing loss of mice carrying human MIR96 mutations. *Genome medicine*, *16*(1), 121.

Lewis, M. A., Quint, E., Glazier, A. M., Fuchs, H., De Angelis, M. H., Langford, C., van Dongen, S., Abreu-Goodger, C., Piipari, M., Redshaw, N., Dalmay, T., Moreno-Pelayo, M. A., Enright, A. J., & Steel, K. P. (2009). An ENU-induced mutation of miR-96 associated with progressive hearing loss in mice. *Nature genetics*, *41*(5), 614–618.

Li, D., Zhao, H., Cui, Z. K., & Tian, G. (2021). The Role of Nrf2 in Hearing Loss. *Frontiers in pharmacology*, *12*, 620921.

Li, H., Kloosterman, W., & Fekete, D. M. (2010). MicroRNA-183 family members regulate sensorineural fates in the inner ear. *The Journal of neuroscience: the official journal of the Society for Neuroscience*, *30*(9), 3254–3263.

Liu, H., Pecka, J. L., Zhang, Q., Soukup, G. A., Beisel, K. W., & He, D. Z. (2014). Characterization of transcriptomes of cochlear inner and outer hair cells. *The Journal of neuroscience : the official journal of the Society for Neuroscience*, *34*(33), 11085–11095.

Mahmoodian-Sani, M. R., & Mehri-Ghahfarrokhi, A. (2017). The potential of miR-183 family expression in inner ear for regeneration, treatment, diagnosis and prognosis of hearing loss. *Journal of otology*, *12*(2), 55–61.

McGrath, J., Tung, C. Y., Liao, X., Belyantseva, I. A., Roy, P., Chakraborty, O., Li, J., Berbari, N. F., Faaborg-Andersen, C. C., Barzik, M., Bird, J. E., Zhao, B., Balakrishnan, L., Friedman, T. B., & Perrin, B. J. (2021). Actin at stereocilia tips is regulated by mechanotransduction and ADF/cofilin. *Current biology: CB*, *31*(6), 1141–1153.e7.

Mencía, A., Modamio-Høybjør, S., Redshaw, N., Morín, M., Mayo-Merino, F., Olavarrieta, L., Aguirre, L. A., del Castillo, I., Steel, K. P., Dalmay, T., Moreno, F., & Moreno-Pelayo, M. A. (2009). Mutations in the seed region of human miR-96 are responsible for nonsyndromic progressive hearing loss. *Nature genetics*, *41*(5), 609–613.

Mittal, R., Liu, G., Polineni, S. P., Bencie, N., Yan, D., & Liu, X. Z. (2019). Role of microRNAs in inner ear development and hearing loss. *Gene*, *686*, 49–55.

Muglia, M., Citrigno, L., D'Errico, E., Magariello, A., Distaso, E., Gasparro, A. A., Scarafino, A., Patitucci, A., Conforti, F. L., Mazzei, R., Cortese, R., Tortelli, R., & Simone, I. L. (2014). A novel KIF5A mutation in an Italian family marked by spastic paraparesis and congenital deafness. *Journal of the neurological sciences*, *343*(1-2), 218–220.

O'Brien, J., Hayder, H., Zayed, Y., & Peng, C. (2018). Overview of MicroRNA Biogenesis, Mechanisms of Actions, and Circulation. *Frontiers in endocrinology*, *9*, 402.

Otzan, G., Iseever, H., Oguz, F., Atak, M., Ezirmik, E., Guldiken, Y. (2023). Genetic variations in *TAOK1, TMTC4, NTF3,* and *CNTN1* and their association with noise-induced hearing loss. *Kuwait Journal of Science, 50*(2), 12-21.

Pang, J., Xiong, H., Yang, H., Ou, Y., Xu, Y., Huang, Q., Lai, L., Chen, S., Zhang, Z., Cai, Y., & Zheng, Y. (2016). Circulating miR-34a levels correlate with age-related hearing loss in mice and humans. *Experimental gerontology*, *76*, 58–67.

Park, J., & Bird, J. E. (2023). The actin cytoskeleton in hair bundle development and hearing loss. *Hearing Research*, *436*, 108817.

Pierce, M. L., Weston, M. D., Fritzsch, B., Gabel, H. W., Ruvkun, G., & Soukup, G. A. (2008). MicroRNA-183 family conservation and ciliated neurosensory organ expression. *Evolution & development*, *10*(1), 106–113.

Prosser, H. M., Koike-Yusa, H., Cooper, J. D., Law, F. C., & Bradley, A. (2011). A resource of vectors and ES cells for targeted deletion of microRNAs in mice. *Nature biotechnology*, *29*(9), 840–845.

Ranum, P. T., Goodwin, A. T., Yoshimura, H., Kolbe, D. L., Walls, W. D., Koh, J. Y., He, D. Z. Z., & Smith, R. J. H. (2019). Insights into the Biology of Hearing and Deafness Revealed by Single-Cell RNA Sequencing. *Cell reports*, *26*(11), 3160–3171.e3.

Rudnicki, A., Avraham, K. (2012). MicroRNAs: the art of silencing in the ear. *EMBO Mol Med, 4*, 849-859.

Sanders, T. R., & Kelley, M. W. (2022). Specification of neuronal subtypes in the spiral ganglion begins prior to birth in the mouse. *Proceedings of the National Academy of Sciences of the United States of America*, *119*(48), e2203935119.

Sherman, B. T., Hao, M., Qiu, J., Jiao, X., Baseler, M. W., Lane, H. C., Imamichi, T., & Chang, W. (2022). DAVID: a web server for functional enrichment analysis and functional annotation of gene lists (2021 update). *Nucleic acids research*, *50*(W1), W216–W221.

Soldà, G., Robusto, M., Primignani, P., Castorina, P., Benzoni, E., Cesarani, A., Ambrosetti, U., Asselta, R., & Duga, S. (2012). A novel mutation within the MIR96 gene causes non-syndromic inherited hearing loss in an Italian family by altering pre-miRNA processing. *Human molecular genetics*, *21*(3), 577–585.

Soukup, G. A., Fritzsch, B., Pierce, M. L., Weston, M. D., Jahan, I., McManus, M. T., & Harfe, B. D. (2009). Residual microRNA expression dictates the extent of inner ear development in conditional Dicer knockout mice. *Developmental biology*, *328*(2), 328–341.

Suzuki H. I. (2023). Roles of MicroRNAs in Disease Biology. *JMA journal*, *6*(2), 104–113.

Tran, S. C., Jaehne, E. J., Dye, L. E., Wong, J., Bakas, J. S., Gasperoni, J. G., Hale, M. W., van den Buuse, M., Dworkin, S., Grommen, S. V. H., & De Groef, B. (2021). Effect of Pleomorphic Adenoma Gene 1 Deficiency on Selected Behaviors in Adult Mice. *Neuroscience*, *455*, 30–38.

Vatsa, N., Kumar, V., Singh, B. K., Kumar, S. S., Sharma, A., & Jana, N. R. (2019). Down-Regulation of miRNA-708 Promotes Aberrant Calcium Signaling by Targeting Neuronatin in a Mouse Model of Angelman Syndrome. *Frontiers in molecular neuroscience*, *12*, 35.

Vidigal, J. A., & Ventura, A. (2015). The biological functions of miRNAs: lessons from in vivo studies. *Trends in cell biology*, *25*(3), 137–147.

Wang, M., Han, Y., Wang, X., Liang, S., Bo, C., Zhang, Z., Wang, M., Xu, L., Zhang, D., Liu, W., & Wang, H. (2021). Characterization of EGR-1 Expression in the Auditory Cortex Following Kanamycin-Induced Hearing Loss in Mice. *Journal of molecular neuroscience: MN*, *71*(11), 2260–2274.

Wang, Q., Li, W., Cai, C., Hu, P., & Lai, R. (2021). miR-153/KCNQ4 axis contributes to noise-induced hearing loss in a mouse model. *The journal of physiological sciences: JPS*, *71*(1), 28.

Weston, M. D., Pierce, M. L., Jensen-Smith, H. C., Fritzsch, B., Rocha-Sanchez, S., Beisel, K. W., & Soukup, G. A. (2011). MicroRNA-183 family expression in hair cell development and requirement of microRNAs for hair cell maintenance and survival. *Developmental dynamics: an official publication of the American Association of Anatomists*, *240*(4), 808–819.

Weston, M. D., Pierce, M. L., Rocha-Sanchez, S., Beisel, K. W., & Soukup, G. A. (2006). MicroRNA gene expression in the mouse inner ear. *Brain research*, *1111*(1), 95–104.

Wienholds, E., Kloosterman, W. P., Miska, E., Alvarez-Saavedra, E., Berezikov, E., de Bruijn, E., Horvitz, H. R., Kauppinen, S., & Plasterk, R. H. (2005). MicroRNA expression in zebrafish embryonic development. *Science (New York, N.Y.)*, *309*(5732), 310–311.

Wijnholds, J., Chowdhury, K., Wehr, R., & Gruss, P. (1995). Segment-specific expression of the neuronatin gene during early hindbrain development. *Developmental biology*, *171*(1), 73–84.

World Health Organization (2018, November 20). Strengthening capacity for the prevention of deafness and hearing loss. https://www.who.int/europe/news/item/20-11-2018-strengthening-capacity-for-the-prevention-of-deafness-and-hearing-loss

World Health Organization. (2021, March 2). WHO: 1 in 4 people projected to have hearing problems by 2050. https://www.who.int/news/item/02-03-2021-who-1-in-4-people-projected-to-have-hearing-problems-by-2050

Xiang, L., Chen, X. J., Wu, K. C., Zhang, C. J., Zhou, G. H., Lv, J. N., Sun, L. F., Cheng, F. F., Cai, X. B., & Jin, Z. B. (2017). miR-183/96 plays a pivotal regulatory role in mouse photoreceptor maturation and maintenance. *Proceedings of the National Academy of Sciences of the United States of America*, *114*(24), 6376–6381.

Xie, Z., Ma, X. H., Bai, Q. F., Tang, J., Sun, J. H., Jiang, F., Guo, W., Wang, C. M., Yang, R., Wen, Y. C., Wang, F. Y., Chen, Y. X., Zhang, H., He, D. Z., Kelley, M. W., Yang, S., & Zhang, W. J. (2023). ZBTB20 is essential for cochlear maturation and hearing in mice. *Proceedings of the National Academy of Sciences of the United States of America*, *120*(24), e2220867120.

Yin, M., Weng, Y., & Qi, T. (2025). PLOD2 exacerbates cervical squamous cell carcinoma by suppressing p53 by binding to YAP1. *Molecular medicine reports*, *31*(1), 23.